Process-based modelling

Henny A.J. Van Lanen[1], Anne F. Van Loon[2], Niko Wanders[3] and Christel Prudhomme[4,5,6]

[1]*Hydrology and Quantitative Water Management Group, Environmental Sciences Group (ESG), Wageningen University & Research, Wageningen, the Netherlands;* [2]*Water & Climate Risk Group, Institute for Environmental Studies (IVM), Vrije Universiteit Amsterdam, Amsterdam, the Netherlands;* [3]*Physical Geography, Utrecht University, Utrecht, the Netherlands;* [4]*Forecast Department, European Centre for Medium-Range Weather Forecasts (ECMWF), Reading, United Kingdom;* [5]*UK Centre for Ecology & Hydrology (UKCEH), Wallingford, Oxfordshire, United Kingdom;* [6]*Geography Department, Loughborough University, Loughborough, United Kingdom*

Chapter outline

9.1 Introduction

The previous chapters (Chapters 6, 7 and 8) address the use of statistical models in low flow and drought analysis. Statistical models are a kind of mathematical models commonly used to describe time series of data, as well as relationships between time series data and other variables (i.e., a data-driven approach). Another kind of mathematical models, which are used in drought research and applications, are so-called process-based models. These models generate continuous time series (e.g., hydrometeorological outputs) by simulating physical processes (e.g., water flow and storage) using information on physiographic characteristics (e.g., land use) and meteorological drivers (e.g., precipitation, evaporation). Two categories of process-based models can be distinguished, that is, hydrological models and socio-hydrological models. These two categories of models along with their model types are presented in this chapter (Fig. 9.1). When the term 'model' is used in this chapter, process-based models are meant, if not otherwise stated. Simulated time series obtained from these models are used to analyse and predict low flow and drought, as elaborated in other parts of the textbook (Chapters 10, 11 and 13).

In hydrological models (Fig. 9.1, left part) processes, such as interception, snow accumulation and melt, overland flow, soil moisture flow, saturated groundwater flow, and surface water flow are included, as well as the interaction between them (Chapter 3). This results in simulated water flow (fluxes) and storages (state variables) that vary over time. Most process-based models are not (fully) physically based — rather they are referred to as conceptual models — because fully physically-based models originate from partial differential equations describing conservation of mass estimated at the local scale (or laboratory scale) of homogeneous systems (Clark et al., 2015). Such description is not feasible for models covering the entire atmosphere-vegetation-subsurface-water domain of, for example, a sub-catchment, because small-scale physical laws cannot be straightforwardly upscaled to larger heterogeneous spatial units (Beven, 2012; Weiler and Beven, 2015). Hence, hydrological
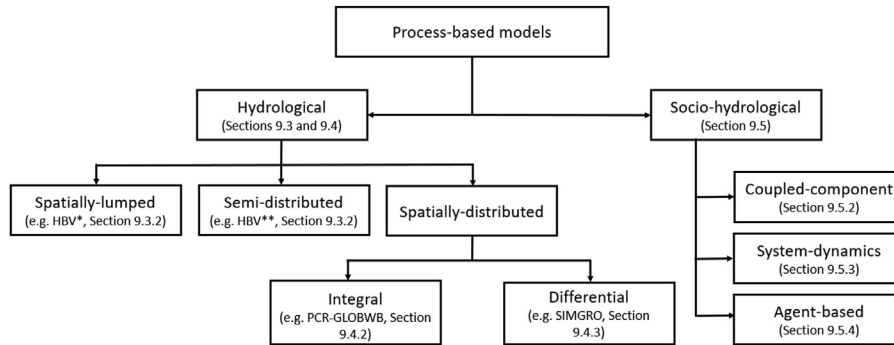
FIGURE 9.1

Process-based models: two categories (hydrological and socio-hydrological), associated model types and example models used in this chapter (HBV is in three versions, lumped, semi-distributed and spatially-distributed (Section 9.2), HBV*, HBV** and HBV*** (Section 9.4.1), respectively). All hydrological model types can be applied as a catchment-scale model or a large-scale model, although lumped models are more regularly used as catchment-scale model. Table 9.1 provides more details.

process-based models are by definition a simplification of reality that contain to varying degrees, conceptual elements (Hrachowitz and Clark, 2017). In order words, these models need to be parametrised, that is, they require a number of parameters that help to conceptualise processes controlling the flow of water and associated physiographic characteristics of the hydrological system.

Water flow and storage in the domain of a hydrological system or model are controlled by both internal and external factors. Internal factors are properties of the material in the model domain (e.g., vegetation, soils, groundwater, rivers), whereas external factors affect the rate at which water enters or leaves the model domain. Internal factors include model parameters, whilst boundary conditions are external factors (e.g., precipitation, river flow, abstractions). Similar to statistical models (Section 7.2), process-based models simulate time series of hydrological variables, for example, river flow, surface water level, groundwater hydraulic head and groundwater discharge, from which drought characteristics and indices can be derived (Chapter 5).

Hydrological models typically simulate the physical system: (a) to improve understanding of its functioning, (b) to naturalise a time series that is influenced by humans, that is, to remove the effect of human interventions (Sections 4.3.9 and 10.4), and (c) to quantitatively explore what happens if people intervene (e.g., abstracting groundwater, building reservoirs) often applying a scenario-based approach (i.e., exploring how the future may develop based on a coherent and internally consistent set of assumptions, including the effect of global change, Section 11.4). Process-based hydrological models are further described in Sections 9.3 and 9.4. However, these models generally only deal with water processes and do not explicitly account for people's response (feedback) to hydroclimatological anomalies or to altered hydrological conditions generated by human interventions.

Socio-hydrological models are required, if people's response needs to be included in the scenario-based approach (Fig. 9.1, right part). These process-based models have been developed to simulate human-water interactions, including feedbacks, as central part of the model. Besides hydrological variables, these models also simulate environmental, social and economic variables, such as water

abstraction rates, reservoir operation schemes, crop yield and income. Simulation of the coupled hydrological–social system, as done with socio-hydrological models, accounts for dynamical interactions between water and people and considers factors, such as long-term socioeconomic (population, prosperity) and water infrastructure developments (Sivapalan et al., 2012). Although the hydrological components of socio-hydrological models usually have a simpler structure than most hydrological models, they play an important role in informing policy makers and water managers by developing a generic understanding of how drought may be enhanced or alleviated from specific interactions between water and human systems (Di Baldassarre et al., 2019). Examples of process-based, socio-hydrological models are further described in Section 9.5. The chapter concludes with some remarks on how to select the best process-based models for drought analysis, including consideration of the associated uncertainty and the purpose of the study (Section 9.6) in addition to data availability.

9.2 Modelling chain: process-based models

First, we describe the whole modelling chain commonly used when process-based models are applied to simulate drought characteristics. Second, how spatial aspects are treated in these models is described, that is, lumped, semi-distributed and spatially distributed models. The section concludes with generic aspects of the calibration and validation of process-based models.

9.2.1 Modelling framework

Process-based models for low flow and hydrological drought analysis are part of a larger modelling chain (data, models, procedures, outputs, Fig. 9.2). As input, models are driven by time series of meteorological data, also referred to as forcing data (Fig. 9.2a). These can be either historical data, going back far in time or representing more recent climate conditions or data describing weather conditions predicted to happen in the next few days (weather forecasting), upcoming months (seasonal forecasting) or decades (e.g., projections up to the end of the 21st century). More details about historical and future drought can be found in Chapter 11, whereas seasonal drought forecasting is elaborated in Chapter 13.

The most reliable meteorological data are those that are observed at a meteorological station. To study catchment-scale drought, this can be a single observed time series from one station or from several stations within or nearby the catchment. For large-scale drought analysis, for example, national, regional or global level, meteorological data from a considerable number of meteorological stations need to be considered. Four categories of large-scale meteorological datasets can be distinguished (Fig. 9.2a, Section 4.4.2.4):

(a) point observations (Category 1) provide time series of meteorological information recorded at in-situ meteorological stations, often not equally distributed across the geographic domain of interest. One example is the European Climate Assessment & Dataset (ECA&D), which contains regularly updated daily data of 13 meteorological variables from around 19,000 stations across Europe (Van den Besselaar et al., 2015)

(b) gridded observations (Category 2) provide time series data over a full domain, generally divided into a regular grid derived from point observations. Examples include E-OBS, a gridded time series dataset at 0.25-degree spatial resolution over Europe generated by interpolating the EC&D
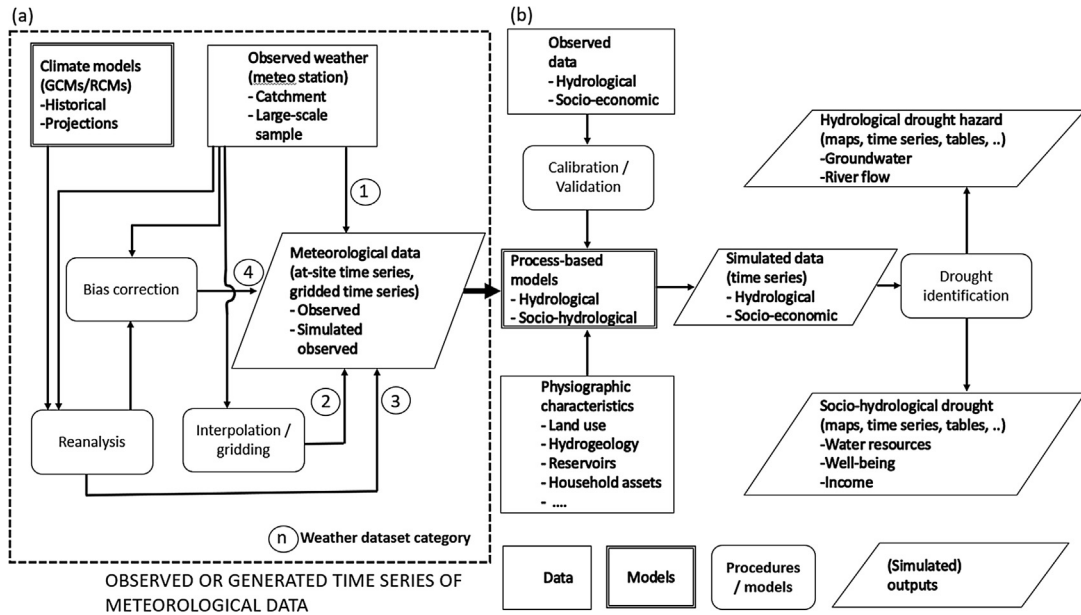
FIGURE 9.2

Modelling chain with its different components (data, models, procedures, outputs) that generates time series of hydrological and socio-economic variables from which drought characteristics can be derived: (a) observed and simulated observed meteorological time series, and (b) process-based models.

dataset (Cornes et al., 2018). A similar dataset is available for the contiguous United States (Newman et al., 2015)

(c) gridded reanalysis (Category 3) is generated using a combination of observations (in-situ, Earth Observations) and models (Box 9.1) to facilitate an extension of the spatial and temporal domain. One well-known example is the Copernicus Climate Change Service ERA5 reanalysis, a global dataset of tens of variables from 1950 to recent (Hersbach et al., 2020)

(d) gridded bias-corrected reanalysis (Category 4) is generated by comparing gridded reanalysis (Category 3) with observation-derived datasets (point or gridded observations, Catogeries 1 and 2) and applying statistical (bias) correction techniques to overcome systematic bias or errors detected in the reanalysis data. One example is WFDE5, a global 50-km dataset generated by applying the WATCH Forcing Data (WFD) methodology (sequential elevation and monthly bias correction techniques) to surface meteorological variables from the ERA5 reanalysis. The WFDE5 is finetuned to force hydrological models (Section 9.4.2.1) to simulate historical periods (Cucchi et al., 2020).

Large-scale gridded meteorological data belonging to Categories 2, 3 and 4 are not directly observed, but the outcome of a mathematical operation (e.g., interpolation or regridding, application of a climate model). Hence, these data are called 'simulated observed' (sometimes proxy or estimated observed) to distinguish from actual observations (Category 1).

Box 9.1 Meteorological data − reanalysis

Reanalysis datasets are based on a collection of meteorological observations from a multitude of sources and provide consistent grids of input data for use in hydrological and socio-hydrological modelling. They combine in-situ ground-based and Earth Observations (EO) and use data assimilation techniques to assimilate these observations into climate models (Fig. 9.2a, Category 3). Observations typically include precipitation, temperature, soil moisture, moisture profile of the atmosphere, sea surface temperatures and different radiation components. Reanalysis seeks an optimal combination of theory (usually in the form of a climate model) with meteorological observations. The climate model, which incorporates physical knowledge of the atmosphere-ocean-land surface system is corrected with relatively limited observed meteorological data. Hence, a reanalysis dataset can be seen as the outcome of pre- and post-processing long-term time series of observational data using a consistent analysis system, including a state-of-the-art climate model. Examples of widely used reanalysis datasets include the ECMWF ERA-interim data (Dee et al., 2011) and ERA5 (Hersbach et al., 2020); NASA's Global Modeling and Assimilation Office MERRA-2 (Gelaro et al., 2017) and Japan Meteorological Agency JRA-55 (Kobayashi et al., 2015). Reanalysis datasets commonly start in the mid-twentieth century and provide seamless spatial grids of time series of meteorological data. Some reanalysis products go back further in time, such as the full twentieth-century reanalysis 20CR (Compo et al., 2011) dating back to 1871. However, the reliability of reanalysis products typically decreases when going back in time as products become more model-based than observation-based due to the sparsity of all observation types (in-situ or EO) before the 1950s. Most reanalysis datasets also include hydrological products, such as gridded time series of groundwater storage and runoff. However, reanalysis datasets are typically simulated from climate models optimised to produce the best meteorological simulations and not the most reliable hydrological outputs. Simulations from hydrological models driven by meteorological reanalysis data are commonly preferred for low flow and hydrological drought analysis rather than using the output from the climate model directly (Fig. 9.2b).

The basic concepts and different types of hydrological and socio-hydrological models (Fig. 9.2b), driven by time series of meteorological data (Fig. 9.2a), are further elaborated in the remaining part of this chapter followed by examples of their application at the catchment scale (Chapter 10 Human influence), at larger scales (continental, global) in Chapter 11 (Past and future hydrological drought) and in Chapter 13 (Drought Early Warning Systems).

9.2.2 Spatial scale of process-based models

Process-based models are here classified based on how they represent the spatial scale:

(a) lumped models
(b) semi-distributed models
(c) distributed models.

Table 9.1 gives an overview of key properties of process-based hydrological models, including how they represent the spatial scale. The terms spatially lumped and spatially distributed are widely applied, often without the prefix 'spatially' (i.e., 'lumped model' or 'distributed model'). In brief, lumped models do not account for the spatial distribution of boundary conditions or model parameters in the plan or map view (Type 1, Table 9.1). Distributed models, in contrast, do account for spatial variability in physiographic characteristics (e.g., different land cover, soils) in the plan or map view (Type 3, Table 9.1), and of boundary conditions, here defined as a prescribed flux or state variable at any point of the top side (e.g., precipitation) and bottom side (usually an impermeable layer is assumed, i.e., flux is zero). A lumped model is effectively a one-dimensional model, as it averages processes over the entire spatial domain or it may include spatial variability only in a probabilistic way and not in a spatially explicit way (see also Section 9.2.3).

Table 9.1 Properties of process-based hydrological models[a].

Type	Spatial nature	Spatial units[b]	Explicit location of spatial unit	Routing of surface water flow to outlet	Lateral groundwater flow between spatial units	Model example	Comment	References
1	(Spatially) lumped	Single	Yes[c]	No	No	HBV*	Single unit version	Bergström (1992), Seibert (2005), URL 9.3
2A	Semi-distributed	Multiple	No[d]	No	No	HBV**	Multiple unit version	Sælthun (1996), Seibert and Vis (2012), URL 9.3
2B			No[d]	Yes[f]	No	Classic, CERF		URLs 9.1. and 9.2
3A	(Spatially) distributed	Multiple	Yes[e]	Yes[g] (most models)	No (integral models)	PCR-GLOBWB, HBV***	Several models, Table 9.2	Sutanudjaja et al. (2018), Wong et al. (2011), URL 9.4
3B			Yes[e]	Yes[g] (most models)	Yes[h] (differential models)	SIMGRO, MIKE SHE, ParFlow		Querner (1988), Van Walsum et al. (2010), URLs 9.6, 9.7 and 9.8

[a]*Models can use one value for each input variable (e.g., daily precipitation) per spatial unit (i.e., deterministic model) or a distribution is used for an input (random component) which results in a distribution for the output (stochastic model).*
[b]*Examples of spatial units are catchments or grid cells (large-scale models).*
[c]*Location of the catchment (spatial unit) is explictly used in the model.*
[d]*Spatial units have no x, y coordinates.*
[e]*Spatial units have explicitly x, y coordinates.*
[f]*Transmission time from the spatial unit to the outlet has been specified, no routing through catchment.*
[g]*Inflow into surface water is specified with x,y coordinates (or grid cell).*
[h]*Lateral groundwater flow between adjacent spatial units is driven by groundwater hydraulic and aquifer characteristics.*
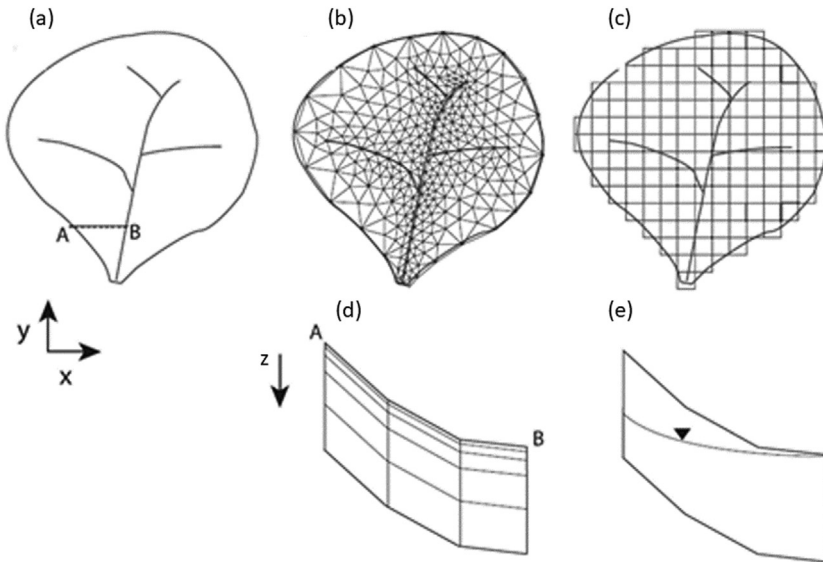
FIGURE 9.3

Examples of model spatial configurations: (a) hypothetical catchment in map view (x,y), (b) TIN discretisation, (c) rectangular grid discretisation, (d) discretisation in depth z, and (e) vertical profile separating unsaturated (above water table) and saturated (below water table) subsurface.

Modified from Kampf and Burges (2007).

The spatial domain can be an individual catchment or water management unit (Fig. 9.3) having three dimensions, with the x and y dimensions representing the land surface and the z dimension representing the depth below the land surface. A lumped model does not divide such a domain (x,y) into separate spatial units, but uses catchment-averaged fluxes (e.g., precipitation, abstractions) and generates average state variables (e.g., soil moisture, groundwater) and fluxes for the entire catchment (e.g., runoff). In a lumped hydrological model, runoff ($L\,T^{-1}$) times the area of the domain gives the total river flow at the outlet in discharge units ($L\,T^{-3}$). Most lumped models generate a single time series for the variable of interest providing a catchment average value (Type 1, Table 9.1). The models generally are deterministic by nature (i.e., one value for each input variable will result in one value for each output variable), although some can be applied in a stochastic mode where a distribution is used for the input variable producing a distribution as output. Some lumped, deterministic models can simulate several time series for a catchment, each representing a distinct land surface type or elevation range, but these are not spatially explicit. These models are referred to as semi-distributed; they divide a catchment into spatial units (Type 2, Table 9.1), representing different physiographical conditions (e.g., elevation, land use, soils). As the spatial units have no specific location in the model domain, there is no lateral interaction between adjacent units (Sælthun, 1996; Seibert and Vis, 2012; URLs 9.1 and 9.2). Lumped and semi-distributed hydrological models are further described in Section 9.3.

(Spatially) distributed models, in contrast to lumped models, do divide the model domain into spatial units with x,y coordinates. In hydrological models, water moves or is routed through the x,y or

x,y,z space (Figs. 9.3b−9.3d), resulting in a two- or three-dimensional model structure (e.g., Kampf and Burges, 2007). The variables are a function of both space and time, which implies that time series for each spatial unit and each variable are generated (Type 3, Table 9.1), generally in a deterministic way (i.e., one value for each input variable is associated with one value for each output variable per spatial unit). Distributed hydrological models are further elaborated in Section 9.4, including specific aspects relative to calibration and validation, whereas more generic aspects are given in Section 9.2.3. Socio-hydrological models can also be lumped or distributed, but are more often distinguished based on how they model human-water interactions (Section 9.5).

In this chapter, the term 'spatial scale' is used to distinguish between lumped, semi-distributed and distributed models (Fig. 9.1). Further, the terms catchment-scale model and large-scale model are also used throughout the textbook. By definition, a catchment-scale model simulates (socio-)hydrological processes in a catchment, which can be anything from a few km^2 to more than $100,000 \ km^2$. Large-scale models commonly cover vast areas, from the national to the continental and global scale. Lumped models are primarily applied as catchment-scale models, whereas distributed models are applied at a range of scales, from catchment to global.

9.2.3 Calibration and validation of process-based (socio-)hydrological models

Most parameters of almost all process-based models cannot be measured directly because they are conceptual entities that need to be calibrated. The scale at which model parameter values are required is generally much larger than the scale of the process or the measurement techniques available. (Socio-)hydrological models can be calibrated and validated in the same way as regression models, that is, model parameters are determined by fitting the model to observations, and the model is then validated against independent data (Sections 7.3.4 and 7.3.6). Quantitative metrics and graphical tools are applied to determine the 'goodness of fit' that measures how well a model can reproduce time series of observed hydrological variables. In hydrology, commonly the simulated time series of discharge are compared against observed discharge at the catchment outlet (Section 4.2.2). Discharge at the outlet represents water outflow from the entire catchment, which makes it very well suited as a target variable for calibration and validation. Several goodness-of-fit metrics are available for model calibration and validation, including the Coefficient of determination (R^2), Nash-Sutcliffe Efficiency (NSE), root mean squared error (RMSE), Akaike Information Criterion (AIC) (Sections 7.5.4 and 7.5.5) and the Kling−Gupta Efficiency (KGE, Gupta et al., 2009). When using process-based models to investigate low flow and hydrological drought, one is advised to apply goodness-of-fit statistics that particularly target the simulation of low flow and groundwater levels. One example being the logarithm of the NSE (^{10}logNSE) because it emphasises the simulation of low river flow rather than the NSE, which puts more weight on the simulation of high flow.

Goodness-of-fit metrics can support the selection of the most suitable model structure, including model parameters. In some distributed models, one can also calibrate initial and boundary conditions (input data or drivers, e.g., set of precipitation stations, different spatial precipitation or groundwater fields). In addition, visualising the differences between simulated and observed times series (residuals) may help to identify model strengths and weaknesses. It provides 'a "feel for how the model operates" (Section 7.3.4) that may be masked by only using goodness-of-fit statistics. In particular, temporal patterns in the residuals (Figs. 7.5 and 7.6) and spatial patterns (for distributed models) can be investigated. When calibrating (socio-)hydrological models an 'objective function' is regularly used.

The objective function (OF) defines which goodness-of-fit metrics (value) is to be minimised or maxised subject to the constrains. For example, Garcia et al. (2017) tested objective functions in their study of low flow for 691 catchments in France using two lumped hydrological models. Several goodness-of-fit metrics, which they called 'assessment criteria', of simulated low flow indices (e.g., Q_{95}, *MAM(3*-day)) were calculated based on NSE, RMSE, and KGE. Among other, six objective functions (OFs) were defined, using one goodness-of-fit metric or combinations of two. It was concluded that OFs using combinations of two goodness-of-fit metrics gave the best model validation results.

Over time, the estimation of parameters of process-based models has been done in several ways; Beven (2012) provides a comprehensive overview. When calibrating a (socio-)hydrological model, one may assume that there exists a single optimum parameter set that best fits the observations. Goodness-of-fit metric(s) of simulations obtained for different parameter sets can be viewed in a 2-D or 3D space (response surface). The search for the global optimum can be done manually by combining expert knowledge (defining reasonable parameter ranges) with trial and error, given that a limited number of parameters are to be calibrated (often considered to be less than 3−5). However, most models have more parameters and then optimisation algorithms (e.g., Mai, 2023) are applied. These build a response surface and seek for the optimum in the goodness-of-fit metric(s), that is, the best performing model. The response surface characterises the 'sensitivity' of model parameters and cannot be visualised for models with more than three parameters. If *n* parameters are involved, the algorithm searches the highest/lowest optimum ('global maximum/minimum') in an *n*-dimensional space. Care should be taken that the algorithm does not get trapped in local optima (Mai, 2023). Some users of multi-parameter models still choose for a manual parameter estimation by only calibrating two or three parameters in one run and keeping the other parameters fixed based on an expert estimate. This step is repeated for another set of 2−3 parameters and proceeds until the parameter values approach stable values without changing the simulated hydrological output variables. Manual calibration of multi-parameter models is generally not recommended because it is hard to account fully for dependencies between parameters. Calibration becomes even more challenging in case of a distributed model where the parameter set may vary per spatial unit (e.g., sub-catchment, grid cell) or cluster of spatial units (e.g., grid cells with same land use). In (socio-)hydrological studies, often insufficient observations are available to find a robust parameter set ('ill-posed' optimisation case), and there is a risk of over-fitting (Section 7.3.6). Although, the goodness-of-fit metric(s) obtained using a single optimum parameter set provide some information on uncertainty, the metric(s) do not give a predictive uncertainty measure (Box. 9.4).

A model using the optimum parameter values (set), as described above, provides the best fit against the observed variable(s) for the chosen calibration period, as defined by the goodness-of-fit metric(s) selected. However, one should realise that all parameter values are affected by possible inadequacies in, for example, model structure, initial and boundary conditions. Likely, a unique optimum parameter set that fits the observations does not exist, and several parameter sets can be equally good ('equifinality'). More comprehensive calibration procedures have been developed to address equifinality. Knowledge using available observed data is applied to define prior parameter distribution functions. Next randomly drawn parameter values are fed into the model, in which the selection of the model structure also requires a critical prior analysis. This step is then repeated numerous times ('Monte Carlo' method, Section 7.2) to yield model results (simulations) in terms of distributions (probabilistic outcome). This implies that there is not one model with a unique parameter set, but several possible

sets that are equally likely. This allows presenting low flow and drought indices also in a distributed way, including the associated uncertainty (Box 9.4). Readers are referred to Beven (2012) for an in-depth discussion of model parameter estimation techniques and potential to quantify associated uncertainty.

Assessing the goodness of fit over a specific calibration period as a way to select the optimum model structure, including model parameters and boundary conditions for a certain region, is not sufficient to describe the predictive power of the model when using it under new conditions (independent data). Model validation is introduced for this reason, which involves examining model performance when using the model for a different (independent) period. The entire dataset is separated into a so-called model-training (calibration) subset and a testing (validation) subset (split sample analysis). In this process of 'cross-validation', one selects the best-suitable model structure, parameter set and boundary conditions based on the training subset and investigates how well this model performs on the (held-out) validation subset. Klemeš (1986) was one of the first presenting an operational framework for spilt sampling in hydrological modelling. This holdout method can be applied several times by splitting the entire dataset with boundary conditions in training and testing subsets covering different sub-periods (*k*-fold cross validation, Section 7.3.6). Robustness of the (socio-)hydrological model can be determined by comparing the goodness-of-fit statistics (R^2, NSE, AIC, RMSE, KGE) of the training subset (calibration sub-period) with those of the testing subset (validation sub-period). One has an acceptable model if the validation statistics are not too different from calibration statistics (acceptable difference is to be defined by the user of the model outcome).

Users of simulation models should realise that the choice of the calibration sub-period affects model performance in the validation sub-period. Consequently, the data splitting scheme is essential in model development (e.g., fine-tuning of model parameters and selection of boundary conditions). Shen et al. (2022) investigated the effect of 50 different split-sample schemes on model performance using about 35 years of data and two hydrological models in hundreds of USA catchments. The total length of the calibration and validation sub-periods varied between 10 and 30 years, leaving 5−25 validation years. The calibration sub-periods (CsP) covered between 30% and 100% of the total record length, that is, calibration sub-periods varied from short-periods to full-periods, respectively. They show that models based on short calibration periods were performing worse than those based on long periods and recommend using the latter as a strategy to obtain robust models. Models using recent CsPs outperform the ones employing earlier CsPs as they better represent the current climate. This means that building a model by calibrating it against the first part of the record (older data) and validating it using the second part of the record (newer data) as a single split-sample analysis, which is not uncommon in hydrological modelling, should be avoided, particularly operating in a non-stationary climate.

Calibration and validation of process-based models that are applied for low flow and drought studies should particularly pay attention to parameters representing storage (e.g., soils, hydrogeology, lakes). In case the model underestimates catchment storage, simulated drought events tend to be too short and occur too frequent. Of key importance are also parameters that control the response to precipitation (e.g., soil infiltration capacity, drainage density). A too high soil infiltration capacity or too low drainage density in the model would lead to simulated streamflow droughts that last too long. The use of lumped models (e.g., HBV, Section 9.3.2) particularly, require care as how to convert spatially distributed information in a catchment to catchment-average physiographic characteristics, considering non-linear responses. On the other hand, distributed models (Section 9.4) are adapted to consider spatially distributed information (e.g., precipitation, land use, lakes), but this implies that

substantially more data are required; data that are adequate and of the required spatial and temporal resolution. Models that are more physically-based, such as SIMGRO (Section 9.4.3), have a higher number of parameters, as compared to lumped models; several of which can be measured or obtained from existing sources, which reduces the numbers of parameters to be calibrated, although the gap between the model scale and the measurement scale still must be bridged. In summary, calibration and validation of process-based models require careful consideration because most likely there is more than one best outcome. Several different models and parameter sets may reproduce the observations equally well and hence, analysing model outcome from a single model with one unique set of parameters, which is not uncommon in low flow and drought model studies (e.g., Sections 9.3.3, 9.4.2, 9.4.3, 9.5.2, 9.5.3, 9.5.4), should be treated with caution.

9.3 (Spatially)lumped hydrological models

In this section, background information on (spatially) lumped hydrological process-based models is presented (Section 9.3.1, Fig. 9.1), followed by an example description (HBV, Section 9.3.2) and application (Section 9.3.3). In Section 10.5.1.1, the model is used to illustrate the impact of human interventions on drought.

9.3.1 Background

Lumped models already have a long history. They represent the model domain as one single column without further spatial discretisation in plan view (x,y in Fig. 9.3a). A common type rooted in holistic empiricism is the 'bucket-type', a conceptual representation of several stores (or buckets) describing the storage of water across the model domain. Examples of stores are snow, lakes, soils and groundwater. Water stored in these buckets represent catchment-averaged storage (Box 9.2).

Box 9.2 Water storage in a lumped model

Subsurface water storage in a lumped model represents catchment-averaged water. The vertical and horizontal exchange of water between the buckets is in most models typically not driven by actual gradients in groundwater hydraulic head, but rather, in a simplified way, exclusively as a function of the water storage in the conceptually hierarchically 'higher' ('above') bucket. For example, the flux describing the percolation from a bucket representing the unsaturated zone (soil bucket) to a bucket representing the groundwater (groundwater bucket) is often formulated exclusively as a function of the water storage in the soil bucket (e.g., Hrachowitz and Clark, 2017). The higher the storage in the upstream bucket, the more water flows to the downstream bucket. The change of storage in a certain bucket i in time step t is:

$$\Delta S_{i,t} = \left(\sum I_{i,t} - \sum O_{i,t} \right) \cdot \Delta t \qquad \text{(B9.1)}$$

$$O_{i,t} = k^b \cdot S_{i,t} \qquad \text{(B9.2)}$$

where: $\Delta S_{i,t}$ change in storage in bucket i over *time step* Δt (L), $\sum I_{i,t}$ is the sum of the inputs from hierarchically 'upstream' buckets ($\mathrm{L\,T^{-1}}$), $\sum O_i$ is the sum of the outputs to hierarchically 'lower' buckets ($\mathrm{L\,T^{-1}}$), k is model parameter representing conductance ($\mathrm{T^{-1}}$), if the expoenent $b = 1$ then the model is linear, and S_i is the volume of water stored (L).

Water input in the hierarchically 'highest or upstream' bucket (external factor) is the catchment-averaged rainfall in non-snow affected climates. In some model structures, buckets have a threshold storage. If the storage exceeds the threshold, the volume of water above the threshold flows (drains) to

the downstream bucket. In most lumped models, the water flux between buckets is one way, implying no water can be flow from lower (downstream) to higher (upstream) buckets. Such models cannot account for capillary rise (no upward flow of water from the groundwater bucket to the soil bucket) or surface water infiltration into an aquifer (no flow of water from the surface water bucket to the groundwater bucket). In lowland catchments, two-ways water flow processes have been introduced not to restrict applicability of lumped models (Brauer et al., 2014).

In this textbook, HBV is selected as an example lumped model (Section 9.3.2). Several other lumped hydrological models exist, of which some are available online as software packages (e.g., Astagneau et al., 2020). Astagneau et al. (2021) describe a unified analysis of eight lumped models from a user' perspective, addressing: (a) the model framework (model structure, adjustable parameters, spatial discretisation, data input and output), (b) practicalities (functionalities, documentation, user implementation), and (c) computation times and R structure (partly or fully coded in R; the latter enables fine tuning to own application). Staudinger et al. (2011) investigated the performance of a series of such lumped models. The models were applied to a Norwegian catchment with both low winter flow (snow-dominated processes) and summer low flow (below-normal rainfall less evaporation). Seventy-nine equally plausible models were built based on different combinations of model components, inclduing fluxes occurring in the upper soil layer and lower soil layer, evapotranspiration (only from upper layer, or from both soil layers), percolation, subsurface flow and surface water runoff. The logarithmic Nash-Sutcliffe Efficiency was used as a goodness-of-fit metric (Section 9.2). Models performed better in simulating winter low flow than summer low flow pointing at different underlying processes (Section 3.7). The authors conclude that it is challenging to satisfactory simulate both winter and summer low flows; only 5% of the models performed well in this Norwegian case. The physical-based nature of most of lumped models is limited (Box 9.3), which challenges their ability to simulate, for example, their response to precipitation after extended dry periods and low river flow that usually stems from slowly-responding storages (e.g., deep groundwater).

Box 9.3 Physical processes in lumped soil-vegetation-atmosphere-transfer (SVAT) models

The soil water atmosphere plant (SWAP) model (Kroes et al., 2017) belongs to the group of SVAT models and is an example of a model that explicitly represents several physical processes. SWAP is a one-dimensional, vertical model that simulates water flow in the unsaturated-saturated column in interaction with vegetation development and subsurface hydrology. Instead of water being transported from a soil bucket to a groundwater bucket (as implemented in most lumped models), the Richards equation for water flow is numerically solved. For the implementation of Richards equation, the soil column in SWAP is subdivided into layers that typically are a few centimetres thick in the topsoil and somewhat thicker in the subsoil. Soil water pressure head difference governs the water flow between the layers rather than the pre-defined functional storage relations (Eq. B9.2). Taufik et al. (2018) provide an example of using SWAP for the assessment of hydrological drought and associated wildfire hazard in humid tropical peatlands.

Lumped models generate catchment-averaged time series of water stored in the different buckets (state variables, e.g., soil water, groundwater) and the water that flows between the buckets (fluxes), which is given a physical meaning, such as percolation, groundwater recharge, base flow, and subsurface flow. The models can be used for systems over a wide range of scales, from the field to catchment scale, if the emergent relationships meaningfully capture the effects of spatial heterogeneity. Some authors (e.g., Fatichi et al., 2016) have criticised lumped models for lacking a robust physical or theoretical basis and for their inability to adequately represent spatial patterns.

9.3.2 The lumped hydrological model HBV

Hydrologiska Byrans Vattenbalansavdelning (HBV) is a well-known example of a spatially lumped, process-based hydrological model (Type 1, Table 9.1, Fig. 9.1) with a conceptual nature (URL 9.3). It was developed in the 1970s at the Swedish Meteorological and Hydrological Institute (Bergström, 1992). Over the years, different versions of HBV have been developed for both research and operational management (Seibert and Bergström, 2022). Although it was originally developed for Scandinavian conditions, the HBV model has been further developed (Seibert, 1999; Seibert and Vis, 2012) and widely used in modelling studies across the world (e.g., Beck et al., 2016). Its successful performance internationally, covering a range of hydrological regimes, is partly a result of its non-linear soil routine controlling the delay and transmission of water input from rain and snow melt (Box 9.2). HBV is chosen as an example lumped model because: (a) it is a rather simple model that is based on water stores (buckets), and (b) it simulates all variables (fluxes, state variables) needed for the investigation of hydrological drought, that is, snow, soil moisture storage, groundwater storage and river discharge. A case study on the impact of groundwater water abstraction on time series of river flow and groundwater levels using HBV is elaborated below. Data are from the Upper-Guadiana catchment in Spain (Section 4.5.3). In Section 10.5.1.1, the example is extended to assess the impact of human intervention on drought in the Upper-Guadiana.

9.3.2.1 Model structure

The structure of HBV is illustrated in Fig. 9.4. The model consists of four components: (a) the snow module, (b) the soil module, (c) the shallow and deep layer storage (modules), also called upper and lower zone, representing fast responding (e.g., shallow groundwater in steep terrain) and slowly responding storages (e.g., deep groundwater layer), and (d) and the routing module. Seibert (2005) comprehensively describes all model equations and parameters.

The snow module simulates precipitation either as snow or rain depending on the threshold temperature (TT). Below this temperature, the precipitation is assumed to fall as snow and accumulates in the snow store. To correct for aerodynamic losses at the precipitation gauge (undercatch) the rainfall and snow fall correction factors (PCORR and SCORR) are introduced. Snow melt is calculated using the degree-day factor (CFMAX), and rain and melt water are retained in the snow store until it exceeds a certain fraction, the water holding capacity (CWH). Liquid water in the snow pack refreezes according to the refreezing coefficient (CFR).

The soil module determines the fraction of rain and snow melt that is stored in the soil bucket or directly recharged to the shallow layer storage. A non-linear relation is used (Box 9.2), and the flux at a given time step depends on the actual water storage of the soil bucket as a fraction of the maximum soil moisture storage (FC) and to the power of the shape coefficient (BETA). Actual evapotranspiration (ET) depends on the potential evapotranspiration (PET) and the evapotransration threshold (LP). If the soil moisture exceeds LP, the actual evapotranspiration equals the potential; otherwise, it is linearly reduced as a function of soil moisture content below LP. The potential evapotranspiration correction factor is used to derive daily potential evaporation rates (PET) from mean monthly values of potential evapotranspiration (PET) and temperature (in the original version of the model). Alternatively, a time series of daily potential evapotranspiration can be used as direct input.

The shallow and deep layer storage are represented by simple linear reservoirs (buckets). The shallow layer storage normally consists of two outflows (Q0 and Q1) depending on the water content (S_{uz})
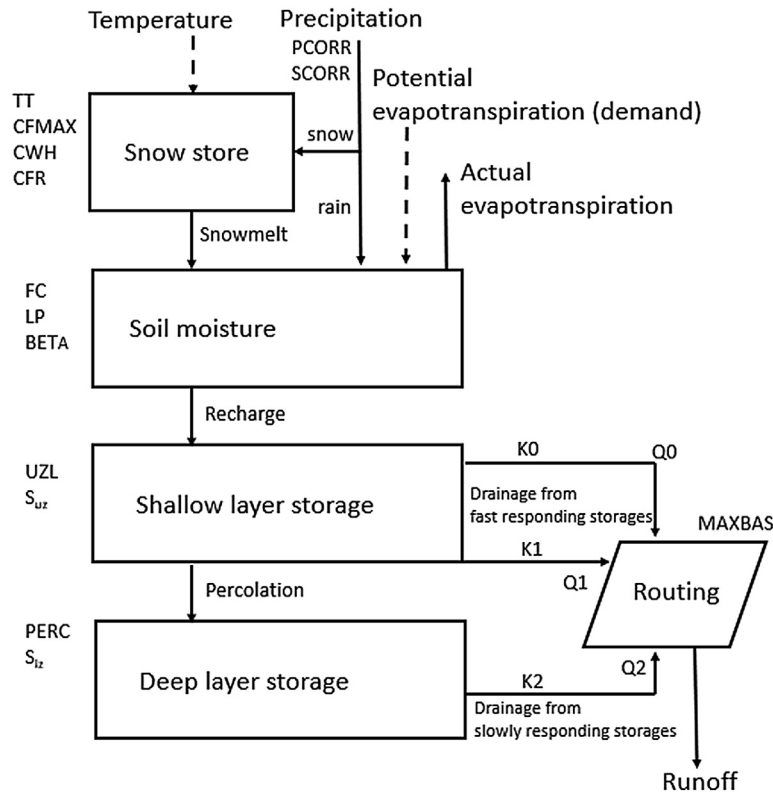
FIGURE 9.4

Schematic overview of the HBV model with the different modules and model parameters. The lumped version of HBV is shown here (HBV*). The model can also be run as a semi-distributed model (HBV**) in which case the snow and soil modules are distributed (Sælthun, 1996; Seibert, 2000). Instead of one time series that feeds the shallow layer storage, there are several recharge time series representing different elevation and vegetation zones in the catchment. In some cases the model is run as a spatially-distributed model (HBV***, e.g., Wong et al., 2011).

and threshold value (UZL), whereas the deep layer storage has one linear outflow (Q2), as shown in Fig. 9.4. Each outflow is linearly related to the recession coefficient (K0, K1, K2) (Section 5.3.4). Water can also percolate from the shallow storage layer to the deep one, depending on the percolation rate (PERC). HBV can also include a lake module next to the deep layer storage (not shown in Fig. 9.4), which directly receives precipitation and loses water through evaporation and outflow. The lake module is connected to the routing module.

The routing module is based on a triangular weighting function defined by the parameter MAX-BAS. It routes the three outflows from the shallow and deep layer storage to the catchment outlet.

HBV can be run either as a lumped or as a semi-distributed model (types 1 and 2A, Table 9.1), that is, the snow and soil modules can be distributed. The catchment can be divided in up to 20 elevation

zones and three vegetation zones (i.e., spatial units, tiles). The elevation zones make it possible to adjust precipitation and temperature due to vertical elevation gradients and are particularly important for snow accumulation and melt. The vegetation zones ensure a unique parameter set for each land cover class reflecting its different physical properties. Every spatial unit obtains a weight that relates its area to whole catchment. Spatial units do not have a specific location in the landscape, that is, not spatially explicit. They can even be different polygons spread over the model domain. Although not spatially explicit, some semi-distributed model versions (URLs 9.1 and 9.2) include an empirical function specifying the transmission time from the spatial unit to the outlet (Type 2B, Table 9.1). Over time, a few alternative model structures for HBV have been developed, as described by Seibert (2005) and Astagneau et al. (2021), including a delay in the response function to mimic delay and flatten groundwater recharge in catchments with thick unsaturated zones (Section 3.3.4.3) and the integration of dynamic glacier melt and geometry change (Seibert and Bergström, 2022). Changes in glacier melt due to global warming may have significant impact on the low flow in summer, increasing the volume of melt water up to a threshold, beyond which the contribution will be reduced due to the decreased glacier size (area and volume) impacting also the overall water resources available for downstream users. The glacial version of HBV can be run as a static model (stationary glaciated area) or as a dynamic model (area is updated every year) (Stahl et al., 2008).

9.3.2.2 Input and output data
The HBV input data comprise (in addition to its parameters), time series of daily catchment-averaged precipitation and temperature (driving forces) for the model period. Precipitation and temperature are corrected for each elevation zone using the vertical precipitation gradient (PCALT) and temperature gradient (TCALT). In addition, precipitation is corrected for undercatch. Furthermore, HBV requires time series of potential evapotranspiration, either daily or monthly average. In the latter case, mean monthly temperature must also be provided. Potential evapotranspiration may be output from any evaporation model, for example, the Penman-Monteith equation. For drought analysis, daily time series of soil moisture and groundwater storage are commonly used, as well as daily river discharge and snow water equivalent, SWE (Wong et al., 2011; Van Loon and Van Lanen, 2012, 2013).

9.3.2.3 Calibration and validation
Although some model parameters of HBV have a physical basis, they are effective only on the scale of the model domain (e.g., catchment), implying that they are hard to measure in the field. That makes calibration of HBV — as all lumped models — necessary. Time series of daily observed river flow for part of the model period are used to calibrate model parameters (Section 9.2.3). The lumped HBV version requires 16 parameters (Fig. 9.4), and hence, it is a challenging to perform an objective and optimum manual calibration. The HBV software package includes tools to perform automatic parameter estimation. Model users can apply the Monte Carlo procedure, which tests thousands of random parameter sets within given parameter ranges to obtain the best sets according to a prescribed goodness-of-fit metric. Another automatic calibration tool available in HBV is based on a Genetic Algorithm (GA, Seibert, 2000, 2005). GA seeks the global optimum (Section 9.2.3) using a random group of different parameter sets as starting point, which then evolves in a way that improves the goodness-of-fit metric until the GA arrives at the global optimum (Beven, 2012).

It is common practice to validate the simulated time series of discharge obtained by the HBV model against observed discharge at the catchment outlet using the split sample approach (Section 9.2.3).

HBV can also be validated by comparing against time series of observed soil moisture and groundwater. However, this is a challenging task, because these observations are site specific (state variables at certain point x,y,z), whereas HBV soil water and groundwater are catchment-averaged values. The inclusion of spatially-distributed observations to get catchment-averaged numbers may provide more realistic data for comparison. In addition, HBV generates stored water in a domain (normally in the unit of mm), which need to be converted into soil water contents and groundwater levels. This extra step requires data, for example, on the storage coefficient of soils and aquifers. In summary, calibration and validation of lumped hydrological models are not straightforward, and care is needed in the interpretation of the results (Section 9.2.3).

Further information on how to use of the HBV model can be found in Seibert and Vis (2012) and at the HBV website (URL 9.3). At the website, one can download the software and an example catchment dataset is provided. One can also find several exercises to get started, and through these get experienced with model calibration, parameter uncertainty and scenario analysis.

9.3.3 Application of the lumped HBV model to the Upper-Guadiana catchment (Spain)

HBV model has been applied to the Upper Guadiana catchment in Spain (Van Loon and Van Lanen, 2013) to assess the impact of groundwater abstraction on hydrological drought (river flow, groundwater level). HBV cannot directly be applied to simulate effects of groundwater abstraction simply because no groundwater gradients are simulated, as in most process-based hydrological models (Section 9.4.1, Table 9.1). However, using HBV to reconstruct natural conditions, that is, without groundwater abstractions, and comparing with the human disturbed (observed) river discharge can help quantify the effect of abstraction on drought (Section 10.5.1.1).

The Upper-Guadiana catchment (16,480 km^2) is located in central Spain, south of Madrid. From this upper part, the Guadiana River flows through western Spain towards Portugal, and drains into the Atlantic Ocean. More details about the Upper-Guadiana catchment and available climate, groundwater level and river flow data can be found in Section 4.5.3.1.

The HBV model developed for the Upper Guadiana incorporated the DELAY extension (Section 9.3.2.1) to account for deep water tables in the catchment (flux across the bottom of soil module is delayed and attenuated before it arrives at the groundwater module). Observed discharge and groundwater levels from the period before intensification of groundwater abstraction (undisturbed period) were used for calibration (1960−70) and validation (1970−80) of the model. The Genetic Algorithm (GA) was used for calibration (Section 9.3.2.3). The Nash-Sutcliffe coefficient (Eq. 7.38) based on the logarithm of the discharge ($^{10}\log Q$) was used as calibration criterion to give more weight to low flow (Section 9.2). Simulated groundwater storage was converted to time series of simulated groundwater levels by introducing a storage coefficient.

Simulated and observed daily river flow for the undisturbed period (natural discharge) are given in Fig. 9.5a. The HBV model simulates the seasonal variability as well as the interannual variability (wet period in early 1960s and dry period mid 1970s) in discharge rather well. Peak flows are underestimated as could be expected given that the calibration gave more weight to the lower flow range (Section 9.2). Simulated groundwater levels are a slightly spikier than the observed, but overall there is a reasonable agreement (Fig. 9.5b). After calibrating and validating HBV on observations from the undisturbed period, the model was run with the observed meteorological forcing from the period with
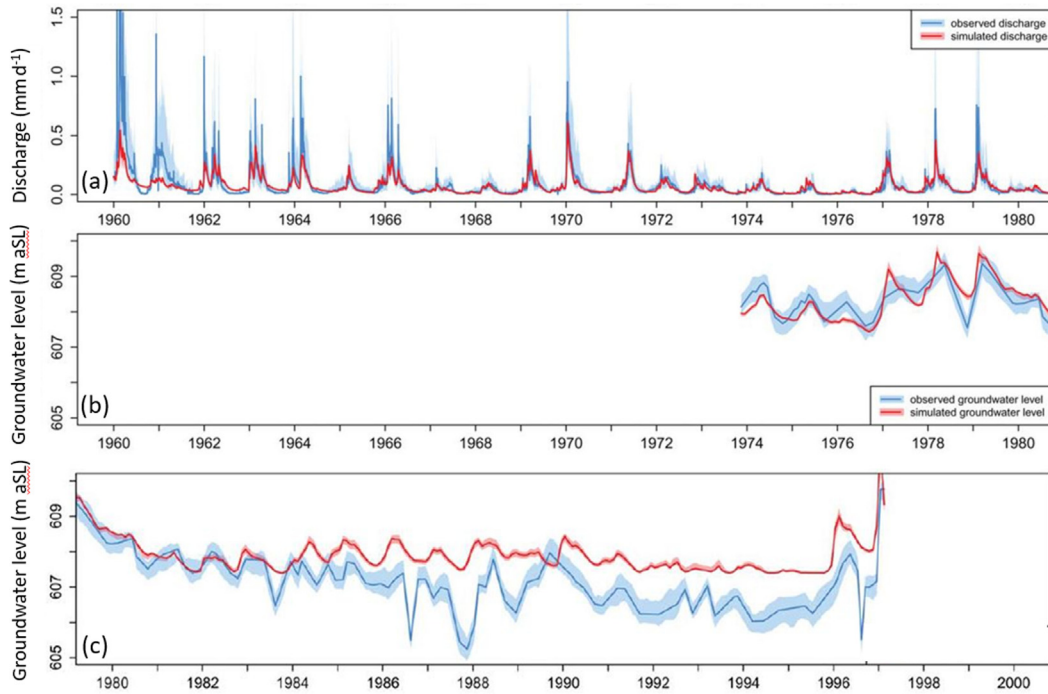
FIGURE 9.5

Observed and simulated hydrological variables in the Upper-Guadiana catchment applying the lumped model HBV for the period 1960—80 without substantial groundwater abstraction (undisturbed) and for the period 1980—2001 with groundwater abstraction (disturbed): (a) discharge at the outlet in the undisturbed period, (b) groundwater level in a representative observation well in the undisturbed period, and (c) in the disturbed period. Uncertainty (*blue shaded areas*) has been added to the observations.

Modified from Van Loon and Van Lanen (2013).

substantial groundwater abstraction (disturbed period) without changing the model parameters. In this way, a so-called naturalised time series is obtained. An example for groundwater is presented in Fig. 9.5c showing the naturalised time series compared with the observed one affected by abstraction. Their difference can then be used to quantify the influence of groundwater abstraction in the Upper Guadiana catchment on hydrological drought (Section 10.5.1.1).

9.4 (Spatially) distributed hydrological models

We start this section with presenting background information on (spatially) distributed process-based hydrological models (Fig. 9.1). Next, two types of distributed models are described: (a) large-scale models that are used to simulate times series of hydrometeorological variables at the global or continental scale (Section 9.4.2), and (b) a catchment-scale model (Section 9.4.3); each with selected example applications. Finally, an introduction to an online self-guided tour demonstrating in a stepwise manner the simulation of the influence of groundwater abstraction using the distributed catchment model is given.

9.4.1 Background

The model domain of distributed models covers a wide range of scales, that is, global, continental, national or regional, as well as catchment-scale models consisting of several sub-catchments. Distributed models explicitly consider heterogeneity within the model domain (Hrachowitz and Clark, 2017). Accordingly, the model domain is divided into spatial units (spatial discretisation). Heterogeneity is accounted for in two ways: (a) spatial units are forced with spatially varying model input (e.g., precipitation, abstractions), and (b) spatially distributed model parameters that account for heterogeneity in physiographic characteristics (e.g., land cover, soil moisture storage capacity, hydraulic conductivity, population density). Commonly, both ways of of accounting for heterogeneity are combined. Spatial units can have different shapes in the plan view. Rectangle shapes (on the relevant spatial projection) are most common, described as 'grids' or 'grid cells', because of their computational efficiency (Fig. 9.3c). Large-scale models often are gridded models, which are aligned with geographic coordinate systems. In some cases, the shape of the model spatial units is governed by the way the water flow equation is solved numerically. For example, gridded models are associated with saturated groundwater models that use finite differences as numerical solution technique. Other models (e.g., surface water flow models and saturated groundwater flow models) may use finite elements as solution technique, which allows to define triangular shapes (Fig. 9.3b). The triangles do not have to be of the same size, which allows flexibility to better represent hydrological similar response units or to make the network denser where head gradients are dense, such as, near rivers (Fig. 9.3b), groundwater abstraction wells, or geological faults.

Spatial distribution in hydrological models also involves the vertical dimension (z, Figs. 9.3d and 9.3e). However, the term spatially distributed model only refers to the spatial discretisation in the plan view (x,y). A fundamental difference among distributed models is, whether the models explicitly simulate lateral groundwater fluxes between neighbouring spatial units (Clark et al., 2015; Hrachowitz and Clark, 2017). Todini (1988) grouped distributed hydrologic models into two broad classes; 'distributed integral models' (Fig. 9.1), defined as a spatial assemblage of one-dimensional column (grid) models, which do not consider lateral fluxes below the soil surface (nGWfl, Section 9.4.2) and 'distributed differential models', which explicitly simulate lateral fluxes of water between spatial units below the soil surface (GWfl) (Section 9.4.3). In nGWfl models, the one-dimensional columns may generate runoff, but there is no lateral flow to neighbouring columns through the subsurface. A water accounting system is used to keep track of the runoff and a routing scheme commonly used to calculate accumulated runoff at specific locations (e.g., river outlets), which is interpreted as discharge. Because GWfl models simulate lateral subsurface fluxes, they require a prescribed flux or state variable at any relevant point of the vertical outsides of the model domain (e.g., groundwater level, surface water level, groundwater flux, river flow) in addition to the boundary conditions at the top and bottom sides (Section 9.2.2). Most large-scale models are distributed integral models. Moreover, several lumped models are also applied as distributed integral model (Type 3A, Table 9.1). For example, the lumped, catchment model HBV (Sections 9.3.2 and 9.3.3) has also been used as a distributed, gridded model (i.e., HBV***) at the national scale (e.g., Wong et al., 2011) and the global scale (Beck et al., 2016).

9.4.2 Large-scale hydrological models

The sub-section presents several large-scale (spatially)-distributed, process-based hydrological models (Fig. 9.1) that have shown to be applicable for drought studies at the global or continental scale. The models have been used for the study of human influences on drought (Chapter 10), the analysis of

historical drought and projection of future drought (Chapter 11) and for monthly and seasonal drought forecasting, as part of an Early Warning System (Chapter 13). In this section, some generic characteristics are presented, some of which are further elaborated in the following chapters (Sections 10.5.4, 11.3.3.3 and 11.4.3), along with a selected example application. This includes the large-scale hydrological model PCR-GLOBWB (Sutanudjaja et al., 2018), which is used throughout for illustration.

9.4.2.1 Historical development

Since the start of the 21st century, large-scale models have been used to explore continental- and global-scale drought (e.g., Sheffield and Wood, 2008; Haddeland et al., 2011; Prudhomme et al., 2014; Wanders et al., 2015; Samaniego et al., 2019). An overview on their background, structure and applicability is described in Van Lanen et al. (2019).

Large-scale models are often classified as land-surface model (LSM) or global hydrological model (GHM). The main difference between the two types is that a LSM focuses on solving the energy balance equation, whereas a GHM focuses on closing the water balance. Both groups vary substantially in complexity among models within one group. Traditionally, LSMs have been developed by the climate community and GHMs by the hydrological community, resulting in a different level of details in modelled processes. Typically, they deviate in the representation of key processes, such as snow accumulation and melt, evapotranspiration components (i.e., canopy evaporation, plant transpiration, soil evaporation, open water evaporation) and the soil module (e.g., number of soil layers and soil parameters represented, runoff scheme). Some LSMs account for the dynamic response of vegetation to the carbon dioxide concentration in the air. Deviations are also found in the generation of runoff and how groundwater and snow are conceptualised (Haddeland et al., 2011). Furthermore, they traditionally deviate in the spatial and temporal resolution, with LSMs normally run at a higher temporal resolution and GHMs at a higher spatial resolution, although recent developments have seen a development towards more similar temporal and spatial scales. Table 9.2 lists several characteristics of large-scale models regularly used in drought studies, as demonstrated in Chapters 10 and 11.

Single large-scale models can be applied to explore particular aspects of hydrological drought. This ranges from reconstructing monthly fields of gridded runoff and soil moisture across Europe over the past (Hanel et al., 2018), to investigate the effect of changing hydrological regime on future drought at the global scale (Wanders et al., 2015), to assess drought risk for both irrigated and rainfed agricultural systems across the world (Meza et al., 2020), and to explore the potential for seasonal hydrological drought forecasting (Sutanto et al., 2020). As demonstrated by these example applications, often an ensemble of (i.e., several) large-scale models are used to provide robust estimates and quantify model uncertainties. Multi-model ensemble (MME) projects have been designed as a community effort to allow intercomparison of hydrological (drought) analyses derived from large-scale model runs (Box 11.2). Following some early initiatives with focus on river flow (Arnell, 2004), more comprehensive assessments have been implemented, such as the Water Model Intercomparison Project (WaterMIP) reported by Haddeland et al. (2011). WaterMIP provided simulated gridded time series of historical and future water balance components from 11 global models (e.g., river runoff, soil moisture, Table 9.2). This allowed the analysis of historical hydrological drought at continental and global scale derived from these time series to be compared (e.g., Gudmundsson et al., 2012; Van Huijgevoort et al., 2013; Tallaksen and Stahl, 2014). In 2012, the Inter-Sectoral Impact Model Intercomparison Project (ISI-MIP) was initiated with a main objective to provide a framework to compare climate impact projections in different sectors and at different scales (Warszawski et al., 2013). An MME of seven large-scale hydrological models (Note: the climate community calls these Global 'Impact' Models, GIMs, Table 9.2, which deviates from our definition of impact models, Section 12.5.1) was the basis

Table 9.2 Characteristics of large-scale models. Extended and updated version from list of models in WaterMIP (Haddeland et al., 2011), ISI-MIP (Prudhomme et al., 2014) and EDgE (Wanders et al., 2019).

Model name	LSM/ GHM	Model time step	Meteorological variables[a]	Energy balance	Evapo-transpiration scheme[b]	Runoff scheme[c]	Snow scheme	Vegetation dynamics	CO$_2$ effect[d]	Included[a]	Reference
GWAVA	GHM	Daily	P, T, W, Q, LWn, SW, SP	No	Penman-Monteith	Saturation excess/Beta function	Degree day	No	No	Water-MIP	Meigh et al. (1999)
H08	LSM	6 h	R, S, T, W, Q, LW, SW, SP	Yes	Bulk formula	Saturation excess/Beta function	Energy balance	No	No	Water-MIP; ISI-MIP	Hanasaki et al. (2008)
HTESSEL	LSM	1 h	R, S, T, W, Q, LW, SW, SP	Yes	Penman-Monteith	Infiltration excess/ Darcy	Energy balance	No	Yes	Water-MIP	Boussetta et al. (2012)
JULES	LSM	1 h	R, S, T, W, Q, LW, SW, SP	Yes	Penman-Monteith	Infiltration excess/ Darcy	Energy balance	Yes	Varying	Water-MIP; ISI-MIP	Essery et al. (2003)
LISFLOOD[e]	GHM	Daily	P, T, ETo, EWo, ESo	No	Penman-Monteith equation/ Hargreaves	Infiltration excess/Beta function	Degree day	No	No		Burek, P. et al. (2013)
LPJmL	GHM	Daily	P, T, LWn, SW	No	Priestley-Taylor	Saturation excess	Degree day	Yes	Varying	Water-MIP	Rost et al. (2008)
MacPDM	GHM	Daily	P, T, W, Q, LWn, SW	No	Penman-Monteith	Saturation excess/Beta function	Degree day	No	No	Water-MIP; ISI-MIP	Gosling and Arnell (2010)
MATSIRO	LSM	1 h	R, S, T, W, Q, LW, SW, SP	Yes	Bulk formula	Infiltration and saturation excess/ groundwater	Energy balance	No	Constant (345 ppm)	Water-MIP	Koirala (2010)
mHM	GHM	Daily	P, Tavg, Tmin, Tmax	No	Penman-Monteith	Saturation excess	Degree day	No	No	EDgE	Samaniego et al. (2019)

Continued

Table 9.2 Characteristics of large-scale models. Extended and updated version from list of models in WaterMIP (Haddeland et al., 2011), ISI-MIP (Prudhomme et al., 2014) and EDgE (Wanders et al., 2019).—cont'd

Model name	LSM/ GHM	Model time step	Meteorological variables[a]	Energy balance	Evapo-transpiration scheme[b]	Runoff scheme[c]	Snow scheme	Vegetation dynamics	CO_2 effect[d]	Included[a]	Reference
MPI-HM	GHM	Daily	P, T	No	Thornthwaite	Saturation excess/Beta function	Degree day	No	No	Water-MIP; ISI-MIP	Hagemann and Gates (2003)
Noah-MP		3 h	P, T, SW, LW, Q, SP, W	Yes	Penman-Monteith	Saturation excess	Energy balance	Yes	—	EDgE	Niu et al. (2011)
Orchidee	LSM	15 min	R, S, T, W, Q, SW, LW, SP	Yes	Bulk formula	Saturation excess	Energy balance	No	Yes	Water-MIP	Guimberteau et al. (2018)
PCR-GLOBWB	GHM	Daily	P, T, ETo	No	Hamon[f]/ Penman-Monteith	Infiltration excess, saturation excess, groundwater	Degree day	No	No	ISI-MIP; EDgE	Sutanudjaja et al. (2018)
VIC	LSM	Daily/ 3 h	P, Tmax, Tmin, W, Q, LW, SW, SP	Snow season	Penman-Monteith	Saturation excess/ Beta function	Energy balance	No	No	ISI-MIP; EDgE	Liang et al. (1996)
WaterGAP	GHM	Daily	P, T, LWn, SW	No	Priestley-Taylor	Beta function	Degree day	No	No	Water-MIP	Alcamo et al. (2003)
WBM	GHM	Daily	P, T	No	Hamon[f]	Saturation excess	Empirical T and P-based formula	No	No	ISI-MIP	Wisser et al. (2010)

[a]*R: Rainfall rate, S: Snowfall rate, P: Precipitation rate (rain or snow distinguished in the model), T: Mean daily air temperature, Tmax: Maximum daily air temperature, Tmin: Minimum daily air temperature, W: Wind speed, Q: Specific humidity, LW: Longwave radiation flux (downward), LWn: Longwave radiation flux (net), SW: Shortwave radiation flux (downward), SP: Surface pressure, ETo: (reference) Evapotranspiration rate, EWo: Potential evaporation rate from open water surface, ESo: Potential evaporation rate from bare soil.*
[b]*Bulk formula: bulk transfer coefficients are used when calculating the turbulent heat fluxes.*
[c]*Beta function: runoff is a nonlinear function of soil moisture or groundwater storage.*
[d]*CO_2 concentration in the air to calculate the stomatal conductance.*
[e]*LISFLOOD was not used in WaterMIP and ISI-MIP, but has been applied for several continental and global studies, incl. forecasting of hydrological drought (Sutanto et al., 2020) and low river flow (Box 13.5) for Europe.*
[f]*see Hamon (1961).*
Modified from: Haddeland et al. (2011). © American Meteorological Society. Used with permission.

for an assessment of future drought in runoff as predicted by five GCMs and four Representative Concentration Pathways (RCPs, Section 11.4.1) at the global scale (Prudhomme et al., 2014). Key results of WaterMIP and ISI-MIP effort with respect to historical and projected water system, including past and future drought, are presented in Chapter 11.

Large-scale hydrological models are also used for seasonal low flow and hydrological drought forecasting. One example is the Copernicus Climate Change Service Sectorial Information System demonstration on water (e.g., Samaniego et al., 2019). Large-scale distributed models (Table 9.2) can also be applied at an intermediate scale, such as the national or regional scale, and they have proven to be key tools for water management at the national scale, incl. managing hydrological extremes (drought and floods). The models can have an integral nature (nGWfl), such as the gridded HBV model (HBV***, spatial resolution 1 km) for the whole of Norway, used to simulate impacts of climate change on hydrological drought (Wong et al., 2011). The models can also have a differential nature (GWfl), for example, the Netherlands Hydrological Instrument, NHI (De Lange et al., 2014). The NHI (smallest spatial unit: 250 m) is a multi-model system for consensus-based, integrated water management and policy analysis in the Netherlands, which also copes with periods of low rainfall, and below-normal river flow and groundwater level. A challenge of distributed hydrological models with a differential nature (GWfl), is the coupling, that is, simulation of a two-way flow between water stores in the unsaturated zone, saturated zone and the surface water system.

9.4.2.2 Model characteristics

Large-scale hydrological models have a spatially distributed nature meaning that they consist of hundreds of thousands vertical 1-D columns (grid cells). Most of these models are integral models (nGWfl). As columns have no subsurface connection, runoff components (surface runoff, base flow) generated in a column are summed and routed based on the topographic gradient to a stream (river cell). The discharge in a certain river cell is the sum of the total runoff from all upstream river cells. Total runoff is routed along the stream network to the catchment outlet (here in the form of discharge). The kinematic wave equation is commonly used to simulate river flow through the stream channel.

The model structure of the 1-D column (grid cell) is similar to that of lumped models (Section 9.3). The PCR-GLOBWB model (Sutanudjaja et al., 2018) is described here as an example of a large-scale model (Table 9.2, URL 9.4) followed by an application. PCR-GLOBWB is one of the ISI-MIP hydrological models (Section 9.4.2.1). The model has a daily *time step* and runs at 5 arcmin spatial resolution (approximately 8 and 4.6 km at 30° and 60° latitude, respectively). Fig. 9.6 presents a schematic overview of the model structure and modules of a 1-D column. The PCR-GLOBWB consists of: (a) meteorological module, (b) land surface module, (c) groundwater module, and (d) surface water module. Spatially distributed precipitation (*P*), temperature and reference evaporation (water loss to the atmosphere from well-watered grass, *E*, Supporting Document 3.1[1]) drive the model. Similar to HBV, reference evaporation may be output from any evaporation model, for example, the Penman-Monteith equation. The land surface module calculates land-cover-specific potential evapotranspiration (*PET*) based on reference evaporation and crop or natural vegetation factors. The degree-day approach is applied to simulate snow melt. The land surface module is the core module and calculates actual evapotranspiration (*ET*) using potential evapotranspiration and soil dryness (*S1*). Furthermore, it simulates snow and interception (canopy) storage, vertical flow among

---

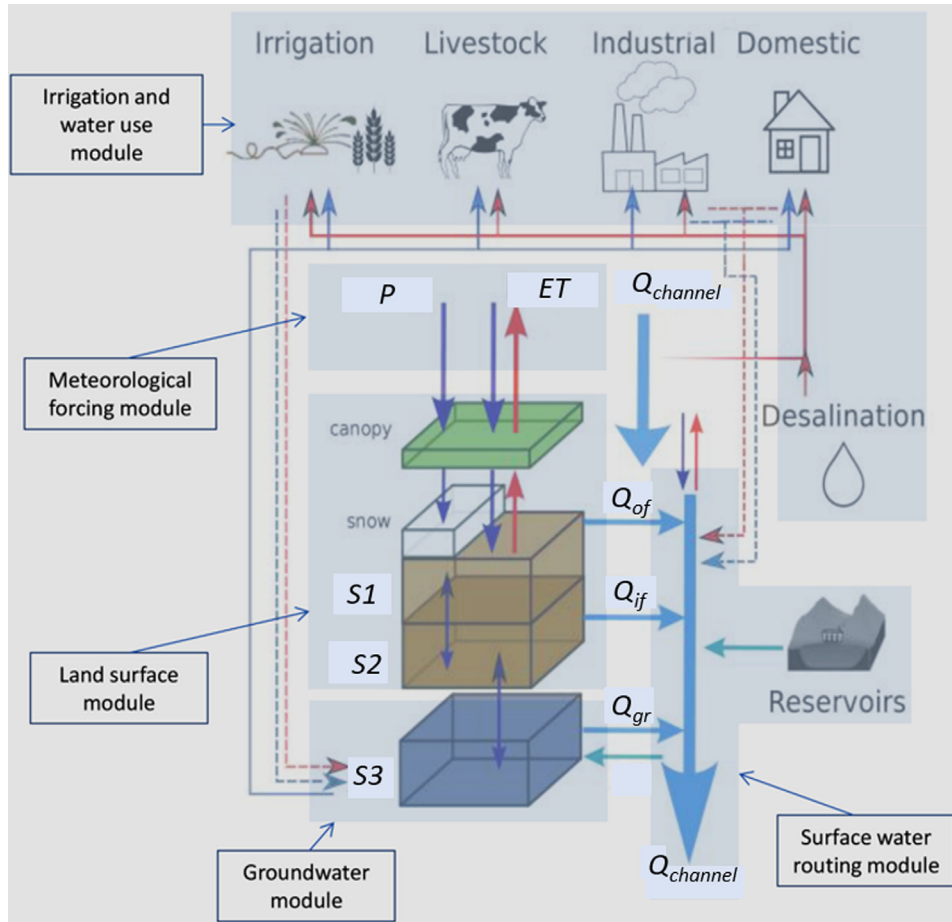[1]https://github.com/HydroDrought/hydrodroughtBook.

FIGURE 9.6

Schematic overview the modules of a PCR-GLOBWB column and its modelled states and fluxes. $S1$, $S2$ (soil moisture storage), $S3$ (groundwater storage), Q_{of} (surface runoff), Q_{if} (interflow or stormflow), Q_{gr} (base flow or groundwater discharge), and riverbed infiltration to groundwater, $Q_{gr} < 0$, takes place when $S3 \leq 0$. The *thin solid red lines* outside the 1-D column indicate surface water withdrawal, the *thin solid blue lines* groundwater abstraction, the *thin red dashed lines* return flow from surface water use, and the *thin blue dashed lines* return flow from groundwater use.

Modified from Sutanudjaja et al. (2018).

soil layers, including capillary rise and groundwater recharge and runoff. These processes are simulated over several land cover types within a model column and aggregated in proportion to land cover fractions. Vegetation characteristics, which may vary over the year, and soil characteristics are unique for each land cover type within a column. This allows a fully spatially distributed specification of vegetation and soils. In the soil, the degrees of saturation of two or three soil layers drive the vertical

fluxes, including groundwater recharge. Surface runoff (Q_{of}, q_{of} in Fig. 3.3 multiplied by the column area) is generated by infiltration excess and saturation excess that considers variable source areas (Section 3.5.1.1) within a column. Interflow (Q_{if}), which can be observed in coarse-grained, partly unweathered soils on hillslopes, is also handled in the same model column. The groundwater module simulates time series of groundwater storage ($S3$) as a response to recharge (or capillary rise) and groundwater discharge (Q_{gr}) (Note: 'transient' means time series of hydrological or socio-hydrological variables — can be input or output from process-based models). If groundwater storage becomes negative, then riverbed infiltration takes place (Q_{gr} is negative). A linear storage-outflow relationship, which depends on drainage network density and aquifer characteristics, is applied to compute groundwater discharge. The groundwater module can be replaced by a saturated groundwater flow model (e.g., MODFLOW) (De Graaf et al., 2015), in which case, the vertical 1-D columns are connected to the nodes of the groundwater flow model. This allows to simulate lateral groundwater flow, groundwater heads and groundwater streamlines. Using a saturated groundwater flow model instead of the groundwater hydraulic flow module, transforms PCR-GLOBWB from an integral model to differential model (nGWfl to GWfl, Section 9.4.1). The surface water module routes the daily total runoff for each column in a catchment to the stream and then along the drainage network until passing the lowermost (downstream) column ($Q_{channel}$). Routing can be simple, that is, accumulating the fluxes over the drainage network or more complex by applying the kinematic wave approach.

PCR-GLOBWB is designed to simulate the effect of human intervention on the water cycle (Bierkens, 2015) and hence, enhancement or alleviation of hydrological drought (Section 10.5.4). The irrigation and water use module (Fig. 9.6) takes water demands, withdrawals and consumption into account. The irrigated area per model column and type of crops grown determine the water demand. Land is irrigated when potential evapotranspiration rates cannot be met by soil moisture storage and precipitation. Water is abstracted either from surface water (fresh, desalinated) or groundwater (renewable and non-renewable). In addition to crop water demands, one can investigate the effects of water required by three sectors: livestock, industry and households (domestic). Data on required water, which may vary over time, need to be specified as input to the model. PCR-GLOBWB also includes a simple reservoir operation scheme (Fig. 9.6), which allows to simulate the impact of over 6000 human-made reservoirs across the globe (stored in the GRaND database, Lehner et al., 2011).

9.4.2.3 Calibration and validation of large-scale models

In contrast to lumped hydrological models (Section 9.3.2), large-scale hydrological models applied at the continental or global scale are hard to calibrate. An important reason is the large number of parameters (in principle each grid cell or model column can have a unique set of parameters). Usually, these models are not calibrated, but in some cases, they are calibrated against observed discharge in large river basins. Performance of large-scale distributed models to simulate low flow or hydrological drought at the level of each grid cell is in most cases lower (Feyen and Dankers, 2009; Van Loon et al., 2012; Tallaksen and Stahl, 2014) than that of well-calibrated lumped models. This particularly holds for regions with large storages (e.g., groundwater, lakes) and in seasonal snow climates. Model structures of large-scale distributed models and lumped models are similar, but less attention is paid to calibration and validation of large-scale distributed models at the grid cell level. There are simply too many grid cells to allow calibration of model parameters for each grid cell individually.

The PCR-GLOBWB model has been calibrated to some extent and validated at length, as reported by Wada et al. (2013), Sutanudjaja et al. (2014, 2018) and Wanders et al. (2015). Simulated discharge

has been compared against over 3500 gauging stations (Sutanudjaja et al., 2018) from the Global Runoff Data Centre (URL 9.5). Additionally, simulated monthly actual evapotranspiration was evaluated against ERA-40 reanalysis data, and simulated terrestrial water storage has been compared with GRACE satellite data. Models with an integral nature, such as PCR-GLOBWB, cannot directly be calibrated or validated against groundwater levels as differential models allow (Section 9.4.3). Moreover, only one module (3rd box, Fig. 9.6) represents the groundwater system in PCR-GLOBWB, which does not allow calibration and validation for groundwater hydraulic heads in a multiple aquifer system. Simulated output from PCR-GLOBWB generally shows good agreement with observed river flow in large river basins and satellite soil moisture.

9.4.2.4 Application at the global scale

Similar to lumped hydrological models applied at the catchment scale (Section 9.3.3), large-scale models can be used for scenario analysis. An interesting aspect of large-scale models is that the effect of different scenarios on low flow or drought can be evaluated spatially across, for example, continents or globally. This means that different regions can be compared, and the temporal and spatial patterns of a historical drought event investigated in detail. Accordingly, regional differences in climate, geology and socio-economic characteristics and their influence on drought characteristics can be analysed, including how humans affect hydrological drought (Wada et al., 2013; Wanders and Wada, 2015). Below a study on the effects of human water use and reservoirs is introduced.

PCR-GLOBWB was used to simulate daily runoff at the global scale at 0.5-degree spatial resolution (about 50 km, Sutanudjaja et al., 2018) in the framework of ISI-MIP (Section 9.4.2.1). Time series of simulated observed meteorological input (Category 4, Section 9.2) was from WFDEI (Weedon et al., 2014). The model was run for the historical period 1901 to 2016. Two scenarios were defined, namely: (a) natural conditions, and (b) human-influenced conditions. Both scenarios included climate change over the 20th century, that is, it was implicitly included in the time series of forcing data. In addition, human-influenced conditions accounted for the development of land use, water abstractions, irrigation and reservoirs. Time series of simulated river flow under natural and human-influenced conditions are given in Fig. 9.7 for two arbitrarily selected 0.5° grid cells (~ 50 km), that is, in Mexico and Brazil. The grid cell in Mexico is located in the eastern part of the country in the River Filobobos catchment, where land use change was the main human intervention in the 20th century. The grid cell in Brazil, which is located close to the River Banabuiú (east Brazil), is in a region with several reservoirs (Van Loon et al., 2022).

Land use change in Mexico (Fig. 9.6a) had hardly any influence on low river flow in the selected period, if any, the land use change resulted in a slightly flashier hydrograph, that is, in half of the time, it was larger and the other half smaller. As expected, the construction of reservoirs in Brazil led to lower river flow in the wet season and higher flow in the dry season (Fig. 9.6b). This is due to the filling up of the reservoir in the wet season and a slow release of this water during the dry season to sustain downstream water demands. In 70% of the time, the river flow was higher. The effect of other interventions on hydrological drought at the global scale is discussed in Section 10.5.4.

9.4.3 The (spatially) distributed catchment model SIMGRO

Here, (spatially) distributed process-based hydrological models applied at the catchment scale are introduced. The SIMGRO model (SIMulation of GROundwater flow and surface water levels) has been selected as an example of a distributed differential model (GWfl) that generates spatially
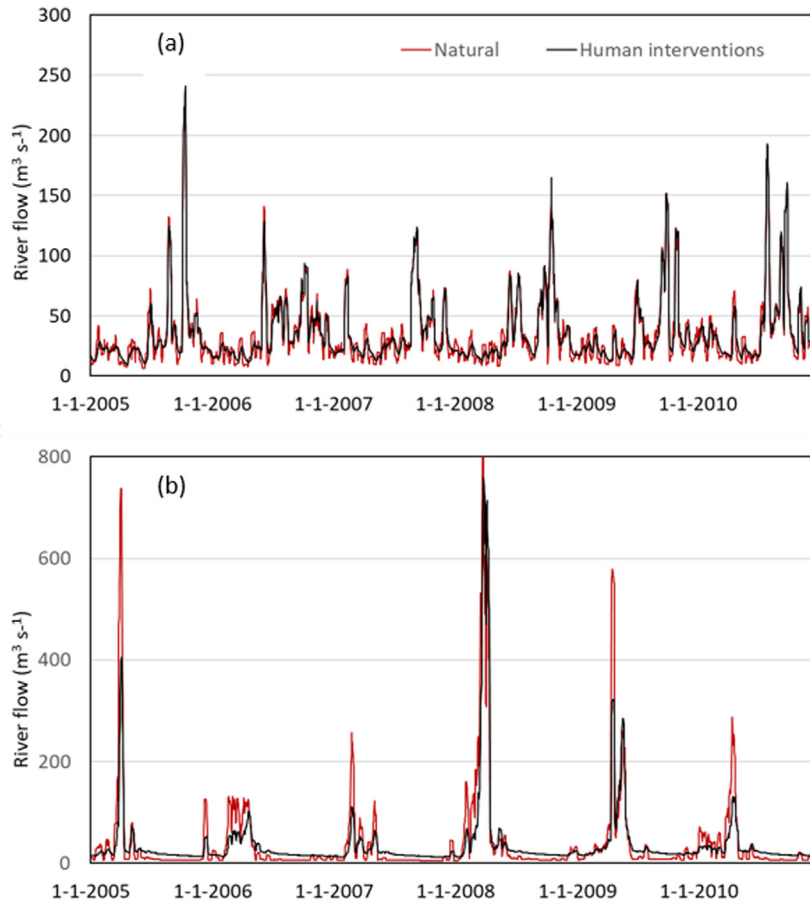
FIGURE 9.7

Simulated river flow (10-day backward moving average) with the (spatially) distributed large-scale model PCR-GLOBWB for the period 2005—10 under natural and human-influenced conditions: (a) Mexico, and (b) Brazil.

distributed time series of hydrological variables both for natural conditions and human-influenced conditions (URL 9.6, Fig. 9.1). Other well-known distributed differential models are the fully inte-grated hydrological model MIKE SHE (URL 9.7) and the ParFlow hydrologic model (URL 9.8). They also fall under the type of 'fully integrated hydrological models' referring to a model structure con-taining all key hydrological domains (vegetation, soil, groundwater, surface water), which dynami-cally interact and solve most flow equations.

9.4.3.1 Model characteristics
SIMGRO is a distributed model of a differential nature (GWfl) that simulates water flow at the catchment scale, implying an explicit simulation of the groundwater (subsurface) flux among spatial units. SIMGRO simulates time series of saturated groundwater flow, unsaturated flow, actual

evapotranspiration, irrigation, river flow, groundwater hydraulic heads (Fig. 3.12) and surface water levels (rivers, channels and lakes) in response to, for example, rainfall, reference evaporation and groundwater abstraction (Querner, 1988; Van Walsum et al., 2010). The model can be applied to catchments or to model domains for which the distributed surface and groundwater boundary conditions (either level or flow) can be specified. It has been applied to catchment area varying from over 100,000 km^2 (Rhine) to a few km^2 (experimental catchments). SIMGRO applies a two-way coupling between modules, i.e., water can flow in both directions. For example, in a spatial model unit water can recharge the saturated zone from the unsaturated zone in one time step (downward flux) and flow upwards (capillary rise) in the next time step. A system of nodal points is superimposed over the catchment delineating so-called elements. The simplest system of nodal points is the well-known regular grid of squares (Fig. 9.3c). SIMGRO, on the other hand, uses triangles to construct the network of nodal points (Fig. 9.3b) allowing input of spatially distributed forcing and catchment properties (e.g., land use, soil type, transmissivity, stream network). SIMGRO simulates multiple aquifer systems (Fig. 9.8 and Section 3.4.1), including interaction between aquifers (leakage or seepage) (Fig. 3.12).
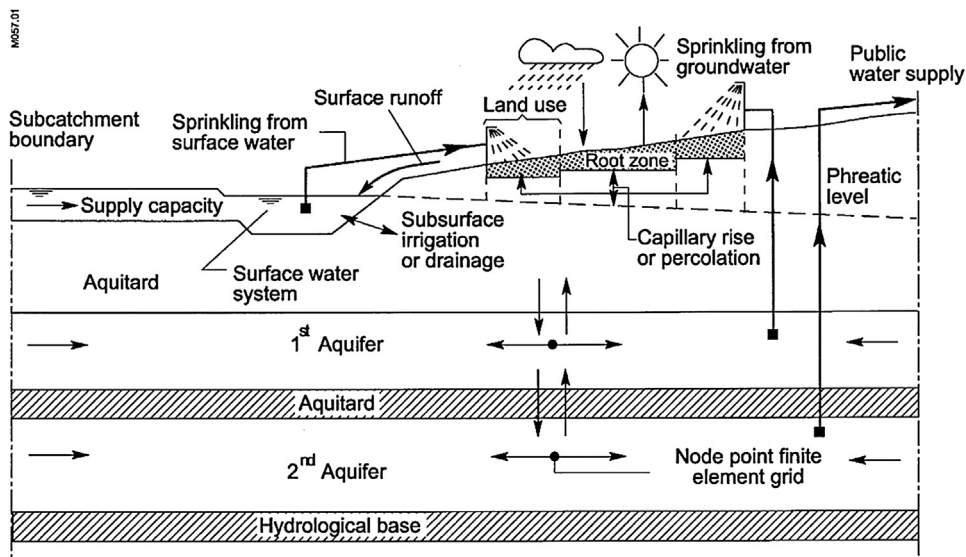

FIGURE 9.8

Schematic overview of water flow in a spatial unit of the (spatially) distributed model SIMGRO (Querner, 1988) in the x-z dimension (y dimension not shown). The cross-section shows the groundwater level (phreatic level) that separates the saturated and unsaturated zone. In this example cross-section, the saturated zone consists from top to bottom of an upper aquitard (i.e., semi-permeable layer), 1st (shallow) aquifer, a deeper aquitard, 2nd (deep) aquifer, and an hydrological base (i.e., impermeable layer). In the shallow and deep aquifer horizontal flow occurs, whereas vertical flow occurs in the aquitards. Groundwater can be abstracted for different purposed (e.g., sprinkling for agriculture, public water supply) from both aquifers. The upper aquitard is fed by percolation from the root zone (upper part of the unsaturated zone) or looses water to the root zone by capillary rise. At the top, the root zone is fed by precipitation (not shown), and sprinkling water that may come from groundwater or surface water (or both). The root zone looses water through evapotranspiration.

Similar to HBV and PCR-GLOBWB, SIMGRO uses time series of daily reference evaporation for a standard crop (grass) as input. This may be output from any evaporation model, for example, the Penman-Monteith equation. The potential evapotranspiration for other crops or vegetation types accounted for in the model, is derived from reference evaporation by converting with known crop or vegetation factors (similar to PCR-GLOBWB). The model assumes steady state in the unsaturated zone for each computation time step (typically 1 day). Important controlling factors are the storage coefficient, S_y, and the capillary rise (negative percolation, q_r) (Fig. 3.3). These depend on soil characteristics (e.g., thickness of root zone, moisture retention, unsaturated hydraulic conductivity, Section 3.3.4.1) and crop data (rooting depth). SIMGRO simulates for each node and time step recharge, I, groundwater hydraulic head, water-table depth and soil moisture storage in the root zone, S_{sor}, and in the unsaturated subsoil, S_{sos} (Appendix 3.1). The model S_{sor} controls actual evapotranspiration per node using a given relationship between soil moisture storage and actual to potential evapotranspiration (ET/PET, Fig. 3.4). SIMGRO distinguishes several drainage sub-systems to simulate the groundwater discharge from the aquifer. These sub-systems represent ditches, and tertiary and secondary water courses. The flow from (or to, as riverbed infiltration is possible) the aquifer is simulated for each drainage sub-system separately using their specific resistance (similar to reciprocal of conductance) and the difference between groundwater level and surface water level. A primary system can also be included in specific nodes ('river nodes') to represent the larger streams in a model domain. River nodes' main function is to convey water, although they also drain groundwater or infiltrate surface water into the aquifer (riverbed infiltration). SIMGRO simulates the surface water system as a network of so-called model surface water reservoirs. The inflow to a reservoir represents outflow from upstream reservoirs and the discharge of the several drainage sub-systems, overland flow and/or water from a sewage treatment plant in the nodal area in which the model reservoir is located. The outflow from the reservoir is the inflow to the next reservoir. Irrigation is driven by soil moisture storage in the root zone. When the storage is below a pre-defined level, a pre-defined volume of water is abstracted (from groundwater or surface water) and applied to land to be irrigated. Water can also be abstracted for domestic water supply. A comprehensive description of the SIMGRO model is provided online (Supporting Document 9.1[1]).

9.4.3.2 Calibration and validation

Distributed models with a differential nature (GWfl), such as SIMGRO, can be calibrated and validated against observed river flow and soil moisture storage at different locations in the model domain (Section 9.2). This is similar to distributed models with an integral nature (nGWfl) and different from the lumped models, which only provide catchment-averaged state variables (Section 9.3.2). The main difference between the two types of distributed models (GWfl versus nGWfl) is that models with a differential nature can be calibrated and validated against observed site-specific groundwater hydraulic heads (x,y,z) in a multiple aquifer system with aquifers on top of each other (Fig. 3.12).

The SIMGRO model was calibrated with observed data from the period 1990−92 with focus on low flow. Actually, a longer period is preferred for calibration, but it is not uncommon for fully integrated hydrological models to have a short calibration period as more than one type of hydrological variable is available (here: groundwater levels at different locations is used in addition to river flow). The simulated flow hydrograph and the flow duration curve, along with time series of groundwater levels from several groundwater observation wells were compared against observed flow and groundwater levels in both catchments. The model was validated using observed data from 1993−95. The model shows good performance especially in the low flow range. Simulated groundwater level mostly deviate less than 0.20 m from the observed level. More details on the calibration and the

validation can be found online (Supporting Document 9.2[1]). More calibration and validation results of the SIMGRO model for the two Dutch catchment is available online (Supporting Documents 9.2[1]).

9.4.3.3 Application to Poelsbeek and Bolscherbeek catchments (the Netherlands)

The SIMGRO model has been applied to the Poelsbeek (41 km^2) and Bolscherbeek (23 km^2) catchments in the eastern part of the Netherlands to investigate the influence of human intervention on drought (Querner and Van Lanen, 2001). The key findings of the study are presented here. The Poelsbeek and Bolscherbeek are adjacent catchments. Shallow water tables and rather wet soils are common. About 75% of both catchments is used as agricultural land; the remaining land is covered by woodland (16%) and residential area (8%). The catchments include an unconfined aquifer with a thickness of 10−60 m overlying impermeable deposits. There is a dense network of streams draining the groundwater system and convey the drained water to the rivers, i.e., Poelsbeek and Bolscherbeek. A more comprehensive description of both catchments is provided online (Supporting Document 9.3[1]).

The period 1951−98 was used as reference (benchmark) for the simulation of distributed recharge, groundwater levels and discharge at the outlet of both catchments. Precipitation varied from 498 to 1218 mm year^{-1} with 10% of the years having less than 595 mm year^{-1}. Potential evapotranspiration varied between 365 and 476 mm year^{-1}, and in 10% of the years, the potential evapotranspiration exceeded 465 mm year^{-1}.

Time series of simulated groundwater levels of one location in the Poelsbeek catchment is given in Fig. 9.9a. In this lowland catchment, the water level fluctuated by about 1.5 m, with dry periods in the late 1950s, the early and mid-1970s, and the mid-1990s. The annual discharge both for the Poelsbeek and the Bolscherbeek catchments are shown in Fig. 9.9b. The average annual discharge of the Bolscherbeek was higher (483 mm year^{-1}) than that of the Poelsbeek (237 mm year^{-1}) due to the effluent of sewage from the town Haaksbergen located in the eastern part of the catchments (source of the town' domestic water supply is outside the catchments). In 10% of the years, the discharge in the Poelsbeek and Bolscherbeek catchments were smaller than 108 and 303 mm year^{-1}, respectively. Dry years in the Poelsbeek catchment (discharge <125 mm year^{-1}) were 1953, 1959, 1971, 1976, 1990, 1995 and 1996 (low discharge in the Bolscherbeek catchment was affected by the effluent of the
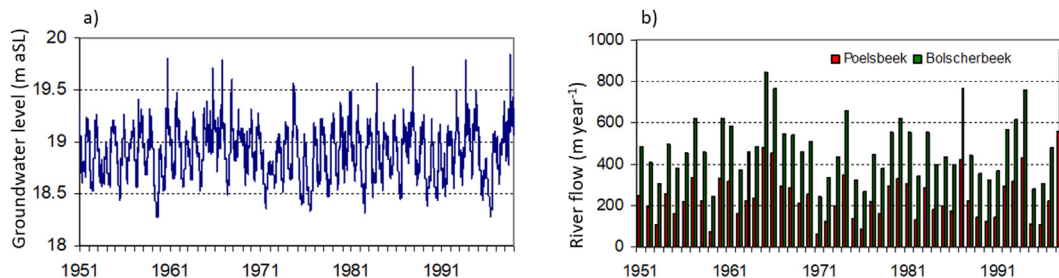

FIGURE 9.9

Simulated time series of hydrological variables with the distributed SIMGRO model in the Poelsbeek and Bolscherbeek catchments (the Netherlands) for the reference period 1951−98: (a) groundwater level at a central location of the Poelsbeek catchment, and (b) annual river flow in both catchments.

sewage plant and thus not reported here). More results for the reference situation, including drought characteristics can be found online (Supporting Document 9.4[1]).

In the Poelsbeek and Bolscherbeek catchments, there was limited groundwater abstraction during the period of study, but this may change in the future in response to increasing water demands. Two potential groundwater abstraction scenarios were defined for the Poelsbeek catchment:

(a) constant abstraction rate of 2050 m^3 day^{-1} during the winter season (October–March) (scenario 05Y, Scen 05Y)

(b) constant abstraction rate of 2050 m^3 day^{-1} throughout the whole year (scenario 1Y, Scen 1Y).

In the simulation, groundwater was abstracted from one single well in the Poelsbeek catchment implying that the influence on groundwater levels in Poelsbeek is larger than in the Bolscherbeek catchment, resulting in lower groundwater levels close to the pumping site during the dry season (Fig. 9.10). Clearly, permanent abstraction (1Y) results in larger drawdowns than only winter abstraction (05Y), but due to non-linear hydrological processes, the 1Y scenario is associated with drawdowns more than twice as large as those for the 05Y scenario. In Section 10.5.3, the simulated river flow and groundwater levels with SIMGRO are discussed further with respect to the influence of abstractions on drought.

Distributed differential hydrological models, such as SIMGRO, can simulate distributed effects of several types of human interventions in which groundwater flow (not only groundwater storage) plays an important role. One example being the effect of a change in groundwater recharge or abstraction in higher-elevation areas (recharge areas) on lower-lying areas in the catchment (discharge areas, Section 3.4.2). A variety of other scenarios can be simulated with SIMGRO. For example, surface water reservoirs can be added, abstractions from groundwater and surface water can be implemented, land use can be changed, return flows can be added or removed and drainage pathways can be altered (higher or lower surface water levels, and reduction of drainage density by removing water courses).
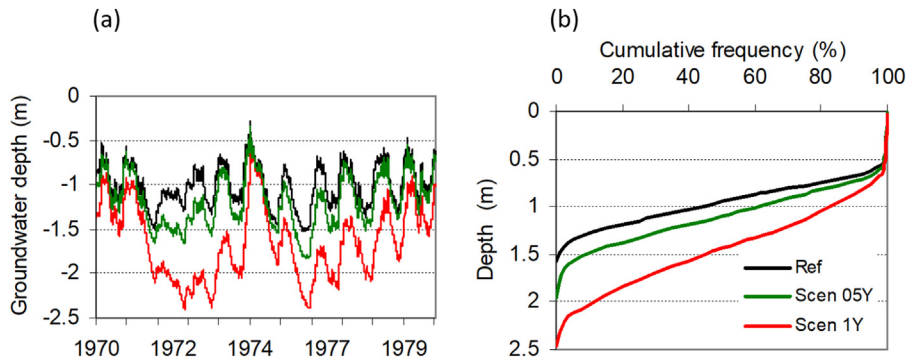

FIGURE 9.10

Simulated groundwater levels with the distributed SIMGRO model for the natural situation (Ref, benchmark) and for the two groundwater abstraction scenarios (Scen 05Y and Scen 1Y, see text) at a location 500 m from the abstraction well in the Poelsbeek catchment: (a) depth to the groundwater level (period 1970–80), and (b) cumulative frequency distribution of the groundwater level (period 1951–98).

9.4.3.4 Self-guided tour: groundwater abstraction in Poelsbeek and Bolscherbeek catchments (the Netherlands)

An online self-guided tour[1] was compiled to demonstrate how to develop a SIMGRO model, and how it can be applied for studies on the influence of human interventions on drought (Section 10.5.3). The example is menu-driven and supports the navigation through the whole assessment procedure. The user works through the procedure at an individual pace and may review or skip a section.

The development of the SIMGRO model and the assessment of the effect of groundwater abstraction in the Poelsbeek and Bolscherbeek catchments on hydrological drought is used as an example to facilitate the learning process. Based upon the practical example, the user learns about: (a) principles of distributed hydrological models with a differential nature, such as SIMGRO, (b) how to perform a model simulation, (c) how to derive and select characteristics of the Poelsbeek and Bolscherbeek catchments, (d) translation of catchment characteristics to model input data, (e) model calibration and validation, (f) drought analysis using the results of a distributed model, and (g) the influence of groundwater abstraction as compared to the natural situation.

At the bottom of the main menu, there are five key buttons: (a) aim, (b) study area, (c) method, (d) model, and (e) scenario. These buttons allow jumping between sections. At the bottom, right two arrow buttons help navigate through a particular part of the procedure. Throughout the exercise, results are discussed, and conclusions drawn. It is important to note that the self-guided tour is not designed to develop a SIMGRO model for the Poelsbeek and Bolscherbeek catchments. The model was already developed and applied, and only results of the study are included in the self-guided tour.

9.5 Socio-hydrological models

9.5.1 Background

Socio-hydrology focuses on linking humans and water in a coupled hydrological-social system (Sivapalan et al., 2012). Fig. 9.11 schematically shows the socio-hydrological cycle, in which changes in hydrology affect society and the other way around. There has been a rapid development in the field of socio-hydrological modelling (Blair and Buytaert, 2016; Srinivasan et al., 2017; Wada et al., 2017), although it is still a rather young field. In contrast to the hydrological models that include some human interventions, such as groundwater abstraction in SIMGRO (Section 10.5.3) or reservoirs in PCRGLOB-WB (Section 10.5.4), socio-hydrological models allow for dynamic changes in the water management. Socio-hydrological models are better suited to describe long-term interactions between
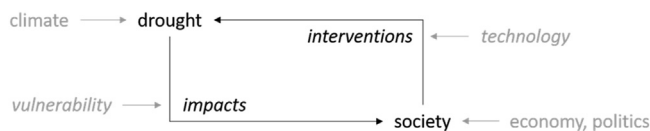

FIGURE 9.11

Feedbacks between drought and society. Climate variability causes drought, which may lead to impacts. Vulnerability determines how these are perceived and influences society. Society (economy and access to technology) governs if and which interventions are taken that aim to alleviate the climate-induced drought.

Modified from Di Baldassarre et al. (2016).

hydrology and human actions, in both water management and policy, but they often do not simulate all hydrological processes at daily timescales.

There are different types of socio-hydrological models as defined by Blair and Buytaert (2016). Here, we focus is on those most used for drought analysis (Fig. 9.1), namely: (a) coupled-component modelling, (b) system-dynamics modelling, and (c) agent-based modelling (ABM). Coupled-component socio-hydrological models (Section 9.5.2) are most similar to the family of hydrological models (Sections 9.3 and 9.4) because they take a hydrological model and couple it to models of social systems, including feedbacks between the model components. In this way, disciplinary models (e.g., water demand models) can be integrated with a hydrological model to form an integrated model for the human-water system. Coupled-component models and system-dynamics models (Section 9.5.3) use a top-down approach. System-dynamics models simulate overall system behaviour based on understanding of the processes connecting system components. Similar to coupled-component models, agent-based models (Section 9.5.4) may also be built including disciplinary (e.g., hydrological) models, but their focus is on the decisions and actions of individual 'agents' within a system. These agents can be individuals (e.g., farmers), groups of individuals (e.g., groups from different sectors) or organisations (e.g., governments, NGOs, businesses). By modelling the behaviour of individual agents and discovering the emerging socio-hydrological patterns, ABMs use a bottom-up approach of modelling the human-water system. The advantage of bottom-up modelling is that real-life complexities are included, and assumptions are based on data, however, this is also its disadvantage, that is, a lot of data are needed to parameterise and validate the models. Therefore, ABMs are often applied on small scales (community or district level). Coupled-component models can be applied from very small (plot) scales to very large (global) scales. The advantage of top-down modelling, such as system-dynamics models, is that further dynamics can be included in a holistic way, and its disadvantage is that it is challenging to parameterise and validate them. System-dynamics models are applied on larger scales (large catchments or countries).

Not all socio-hydrological models are applied to an actual case. Some applications of socio-hydrological models are completely theoretical or based on some real-life situations, but then generalised to the point where the model does not match any situation on the ground, for example, taking some characteristics of the system as starting point for the model setup and then make it generic or averaging characteristics from different cases into one.

9.5.2 Coupled-component models

Coupled-component models used for socio-hydrology connect a hydrological model with a model that simulates human activities. The most common coupling is with a crop model that includes, for example, irrigation, planting of different crops or applying different soil improvement measures (e.g., McNider et al., 2015). Hydrological models can also be coupled to economics models as done for flood risk (e.g., Falter et al., 2015), environmental flows (e.g., Akter et al., 2014) or decision-making models including water demand and supply (e.g., Giuliani et al., 2016). Alternatively, many different models can be combined in a model system or chain that resembles large-scale earth system models (e.g., Barthel et al., 2012). The main difference between impact models, such as those used in ISI-MIP (Section 9.4.2), and socio-hydrological coupled-component models, is that the latter include dynamic feedbacks from the social or economics components back to the hydrological system. The degree of integration differs, depending on how similar the models are in terms of their setup (lumped

versus distributed, Section 9.2). Because disciplinary models are used as starting point in coupled-component models, a basic understanding of key processes within each discipline is included by default. However, this also means that different types of data are needed to parameterise the combined model, and uncertainties of the different model components may escalate because of non-linear effects.

9.5.2.1 Calibration and validation

Coupled-component models can be calibrated as a combined model or separately for each component. For example, Maneta et al. (2009) calibrated the hydrologic and economics parts of the model framework independently. In either way, calibration of coupled-component models is complex and data-intensive. Especially socio-economic data are often not available or not in the time resolution needed or at the correct spatial scale. More commonly, coupled-component models are calibrated on only one component of the coupled system (e.g., McNider et al., 2015 on crop yield, Falter et al., 2015 on river discharge). However, more often, they are not calibrated, only validated or neither calibrated nor validated. No — or partial — calibration is often considered acceptable when the models are used for assessing relative differences between scenarios (e.g., Barthel et al., 2012), but it does question the suitability for accurately representing real-world systems.

9.5.2.2 Application

A coupled-component model experiment is here demonstrated investigating the interaction between drought management, groundwater abstraction and drought (Fig. 9.12) through the coupling of a hydrological model with a water demand component. The example is based on the work of Wendt et al. (2021).

In Fig. 9.12, the two-sided arrows, between the water demand component and the groundwater and surface water reservoir components, represent the feedbacks included in the model. In this example, the hydrological model components (soil water, surface water reservoir, groundwater) are based on common hydrological model structures, and the water demand component is developed from a review of water resource and drought management plans (Wendt et al., 2021). The coupled-component model is set up to represent general hydrological conditions and drought management in England, but is not specific for one location. Input data and model setup are based on typical average conditions for climate, hydrogeology and drought management measures. The model is not calibrated or validated and is used to analyse effects of different drought management strategies on hydrological drought as further elaborated in Section 10.5.6.1.

9.5.3 System-dynamics models

To study feedbacks between drought and people, a flexible and top-down modelling approach, such as system-dynamics can be useful. The social aspects in these models, such as vulnerability, awareness and memory, are hard to quantify or measure. Still, the models play a key role, for example, in determining the relationship between low flow, hydrological drought and societal impacts. Social aspects are important to understand as they may explain non-linearities in the system as a result of unexpected system behaviour. For example, consecutive droughts can make a society vulnerable if it reaches a tipping point (an irreversible system change due to a series of small changes or incidents). The development of a system-dynamics model starts with a conceptualisation of the human-water
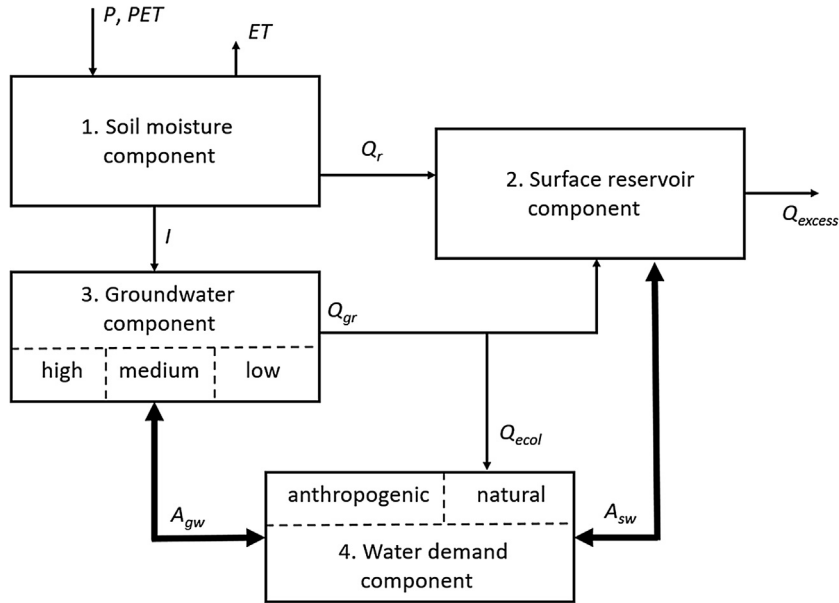
FIGURE 9.12

Setup of a coupled-component model with the soil moisture component (1): the water balance is driven by climate input (precipitation (P) and potential evapotranspiration (PET)). Losses are to the atmosphere (actual evapotranspiration, ET), through surface runoff (Q_r) stored in the surface water reservoir (2) and as groundwater recharge (I) (Q_r equals q_{of} and q_{if}, Fig. 3.3) multiplied by the area of the model domain. Groundwater component (3): storage is represented in three compartments (high, medium, low storage) generating base flow (Q_{gr}) of which Q_{80} is released as ecological minimum flow (Q_{ecol}, representing natural water demand) before routing the remainder to the surface water reservoir. When the surface reservoir is full, excess water leaves the model (Q_{excess}). Stored surface water and groundwater can be abstracted (A_{sw} and A_{gw}) to meet the anthropogenic water demand. Water demand (4) is always satisfied by a combination of surface water abstraction (A_{sw}) and groundwater abstraction (A_{gw}). Bold arrows indicate the components affected by (modelled) drought measures taken.

Modified from Wendt et al. (2021).

system in causal loop diagrams, which are then converted into a set of non-linear differential equations. The conceptualisations used can be very simple or very complex, depending on the processes deemed relevant for the research question under study. The processes are not modelled in a spatially explicit way, so system-dynamics models can be regarded as having a lumped structure (Section 9.2). Blair and Buytaert (2016), Garcia et al. (2016) and the examples presented below provide more information.

9.5.3.1 Calibration and validation

Typically, system-dynamics models are not calibrated. However, there are some examples of system-dynamics models that determine parameter values from observations. For example, Van Emmerik et al. (2014) calibrated parameters of equations representing irrigation and environmental awareness, based

on temporal trends in observed water resources, area under irrigation and population size. Most system-dynamics models are hypothetical or semi-hypothetical, meaning that their setup is based on a generic understanding of a coupled system modelled based on several cases. These models are validated qualitatively to check whether they can represent socio-hydrological shifts that have occurred in the past in a general sense. For example, Di Baldassarre et al. (2013) simulated flooding and adaptation responses (migration, flood protection infrastructure) and compared their model results to typical flood responses observed in floodplains around the world, citing examples from the literature. Garcia et al. (2016) simulated the effects of reservoir operation rules on urban water supply and based their model setup on water supply systems of typical cities in the western United States.

9.5.3.2 Application

System-dynamics models come in very different shapes and forms. Here, a few examples focusing on drought are briefly showcased and further explored in Section 10.5.6.2. Kuil et al. (2016) modelled the collapse of the Maya society. Their model consists of nonlinear differential equations of hydrology, agricultural cropping, population dynamics and reservoir building (Fig. 9.13). Historical understanding of population dynamics, economy, food needs, land and water management were used to set up the model and calibrate some of its parameters.
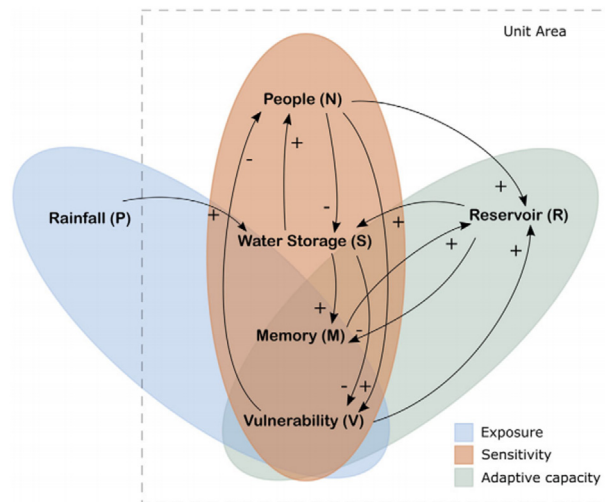

FIGURE 9.13

Flow diagram showing the fluxes and state variables of a system-dynamics model and their ineraction. When P increases, water storage, S, increases, resulting in a higher crop yield (not shown) and population (people, N) can grow. The use of water by the society (people, N) leads in turn to a decrease in storage, S. If population increases, this could potentially lead to a higher vulnerability, V, of the system, although increased water storage, S, would counteract this. Increased vulnerability, V, motivates society to construct reservoirs, R, provided that there are enough people (labour) to do so. More reservoirs allow increased water storage, S. If storage is high relative to the storage capacity, memory, M, is high and reservoir construction, R, continues, but by creating more storage, (people) memory, M, decreases. Lastly, when the system is vulnerable and a certain threshold is reached, population is impacted negatively (Kuil et al., 2016).
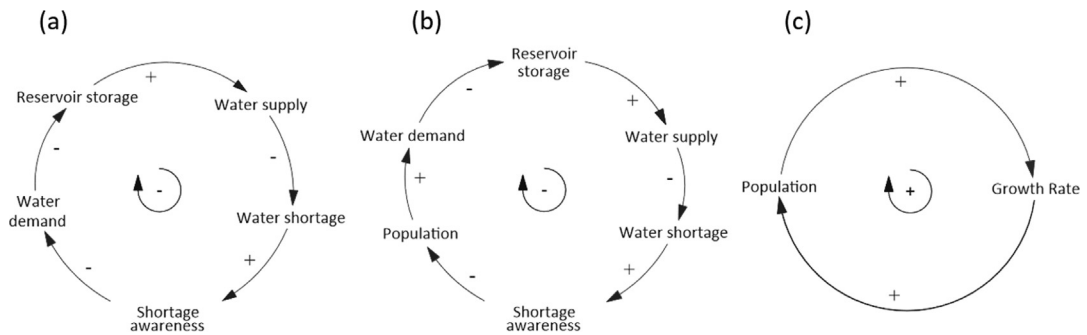
FIGURE 9.14

Causal loop diagrams: (a) water demand, shortage and storage, (b) water demand, shortage and population, and (c) population and growth rate (Garcia et al., 2016).

System-dynamics models are also applied to modern systems. Garcia et al. (2016), for example, used a system-dynamics model to address the question: "What is the impact of reservoir operation policy on the reliability of water supply for a growing city?", analysing the effect of people's response to drought. They conceptualised the model from an understanding of the system using causal loop diagrams (Fig. 9.14) and from typical relationships between the variables being studied. Firstly, a demand for water leads to a lower reservoir storage (Fig. 9.14a), an increase in the water supply, a lower water shortage and an increased shortage awareness that results in lower water demand. The increased shortage awareness leads to smaller population (Fig. 9.14b). Lastly, an increased population results into a higher growth rate and vice versa (Fig. 9.14c).

9.5.4 Agent-based models

Agent-based models (ABMs) have a history in object-oriented programming, cognitive psychology and ecology and are increasingly used to simulate human-water interactions (Blair and Buytaert, 2016; Wens et al., 2019). The strength of ABMs is that they can simulate emergent behaviour or macro-scale effects that arise from interactions between individual agents (e.g., a farmer, household, community, government entity, commercial company) and their socio-economic, policy and natural environment. The development of AMBs requires several steps: (a) definition of the research question, (b) setting of relevant agents and their environment, and (c) definition of behaviour of agents. Their behaviour is characterised by the interaction of agents with each other and with the environment, their decision-making process and their learning capabilities. When those are defined, computational algorithms are developed to represent agents, their environment and individual behaviour. In contrast to coupled-component models and system-dynamics models, ABMs inherently simulate heterogeneous results as the behaviour of agents is individual, and hence, their interaction with their environment is diverse. For example, decisions regarding abstracting water for irrigation depend on each farmer's individual characteristics (e.g., risk perception, financial situation, knowledge) and therefore differ from farmer to farmer, resulting in a spatially heterogeneous abstraction pattern. The interaction with the environment can be modelled in a distributed way, therefore, ABMs can be coupled to distributed disciplinary models of, for example, hydrology (e.g., Castilla-Rho et al., 2015 for groundwater) or

agriculture (e.g., Wens et al., 2020 for crop yield). Similar to coupled-component models and system-dynamics models, ABMs can be set up to represent a real-life situation, or they can be hypothetical, grounded in theory, or in a combination of characteristics of existing cases (e.g., Barreteau et al., 2014).

9.5.4.1 Calibration and validation

Calibration and validation of ABMs are challenging. The procedure is similar to hydrological models (Section 9.2.3). Most commonly, calibration is not done due to the lack of data on behaviour or unique feedbacks are modelled that are hard to observe. If the parametrisation of agent behaviours and their interactions are determined from qualitative data (interviews, questionnaires, focus groups, Section 4.3.9), the model is assumed to represent on-the-ground conditions. Participatory modelling (making use of practical knowledge of individual stakeholders (agents, e.g., Matthews et al., 2007) can be a valuable tool to set up ABMs. Each agent can be interviewed to determine their decision-making preference and then included in the modelling process to make sure the model represents their behaviour correctly. Calibration can be done on some components of the system, especially when coupled to disciplinary models. For example, Wens et al. (2020) calibrated their coupled ABM-crop model on observed crop yields. Similar as in system-dynamics modelling, validation of ABMs is often done qualitatively, checking whether the model outcomes match observed trends in, for example, time series of environmental (e.g., water use) or socio-economic observations (e.g., food insecurity).

9.5.4.2 Application

Many applications of ABMs are focussing on water use in agriculture (e.g., Kuil et al., 2018; Van Duinen et al., 2016). Wens et al. (2020) developed the ADOPT model (Fig. 9.15) to simulate adaptation behaviour of farmers in Kenya to drought. The model is parameterised using data collected from interviews with 250 households and discussions with local decision-makers. The adoption of drought adaptation strategies, such as installing a groundwater well, applying manual or drip irrigation, building terraces and applying mulch, was investigated and linked to economic theories. Such a model allows for testing of scenarios of different farmer behaviours, policy interventions and drought events. What effect the different scenario has on agricultural drought impacts and food insecurity is explored in more detail in Section 10.5.6.3.

9.6 Selection of process-based models to study hydrological drought

It must be accepted that any model, by definition, is a simplification of the real world. It is important to develop models or use model outputs that are as representative as possible, but also to understand the inherited model limitations. Selection of the model that best answers the question being posed is challenging. Benefits and drawbacks of more complex models should be weighed against those from simple models. For example, the choice between a more complex, distributed (socio-)hydrological model versus a simpler, lumped model or the choice between a more complex model that simulates groundwater flow (differential, GWfl) or a simpler model that does not (integral, nGWfl). However, it is not only the model complexity that matters, but also data availability and practicality (e.g., user's knowledge, available software package to build the model, available financial resources, purpose of the study, time to answer the question). (Socio-)hydrological models suited for drought analysis have at least one feature in common, being 'transient' meaning that these models simulate time series of
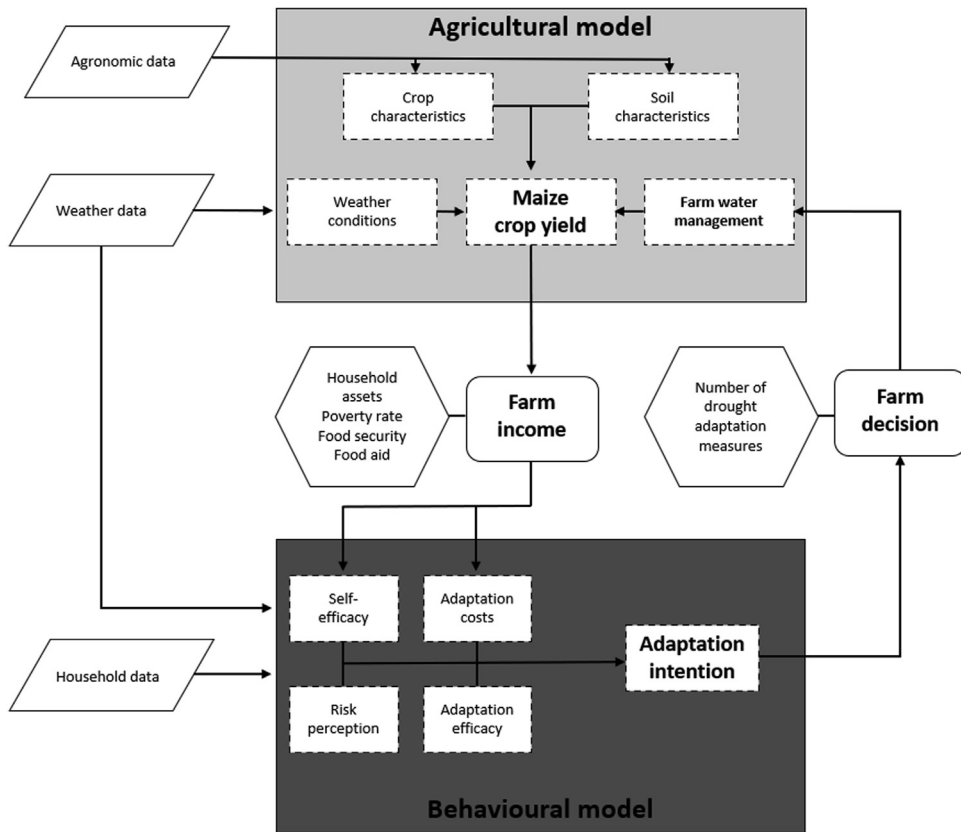
FIGURE 9.15

Modelling scheme of an agent-based model (the agricultural drought risk adaptation model ADOPT):
(a) agricultural model that simulates seasonal maize crop production using weather and agronomic data (light grey box). The resulting household maize crop yield is converted into farm income, and (b) fed into a behavioural model using household data. The adaptation intention is simulated by addressing self-efficacy (individual's belief in their capacity to act in the ways necessary to adapt to drought), risk perception, adaptation costs and adaptation efficacy (dark grey box). The annual decision whether or not to adopt new adaptation measures, influences future on-farm water management, thus creating a feedback. Annual risk indicators (household assets, poverty, food insecurity, food aid) and drought adaptation measures are outputs of the model.

Modified from Wens et al. (2020).

hydrological or socio-hydrological variables. Lumped models are often preferred because they: (a) simplify processes, include a limited number of parameters and hence, are easy to calibrate, (b) are easy to use and no advanced computer skills are required, and (c) are fast and thus less computational demanding (e.g., for forecasting). Whether lumped models are sufficiently fit for purpose depend on the: (a) heterogeneity of the model area, (b) type of question to be answered or physiographic

conditions to be modelled (determining the type of domains and interactions to be represented, e.g., atmosphere-vegetation, unsaturated zone, saturation zone, or surface water), and (c) complexity of the (modelled) interactions between hydrological domains (i.e., what processes need to be represented). Selecting the optimal model type is critical because the outcome of the study depends on it (e.g., Fenicia et al., 2014). Although model choice is fundamental, a study by Addor and Melsen (2018) mining over 1500 peer-reviewed papers, shows that hydrological models are usually not primarily selected because of their adequacy, but because of legacy reasons (e.g., practicality, convenience, experience, custom use). The high number of hydrological models available has led to the creation of meta-modelling frameworks (e.g., Euser et al., 2013), which allow users to evaluate the suitability of various model structures to their need or to combine different process representations. This is the motivation for the Framework for Understanding Structural Errors (FUSE), which provides multiple options for building a hydrological model, including the selection of different process parameterisations for soil layers and conceptualisation of surface runoff, vertical percolation, evaporation and subsurface flow (Clark et al., 2008). Staudinger et al. (2011) applied FUSE to study the performance of a series of lumped models to simulate low flow. A Community Hydrological Model has even been proposed (Weiler and Beven, 2015).

In this chapter, three process-based hydrological models (HBV, PCR-GLOBWB and SIMGRO) and three types of process-based socio-hydrological modelling (coupled-component, system-dynamics, agent-based) are described (Fig. 9.1, Table 9.1) from which the outcome is used to assess the impact of human influences on drought (Section 10.5). These are just examples and clearly many similar models exist that deviate, for example, in: (a) the (socio-)hydrological processes represented in the model, (b) data requirements, (c) lumped or distributed, (d) spatial dimensions, (e) numerical solution method, (f) pre- and post-processors, and (g) computation time. Any low flow or drought project needs to allocate sufficient time to choose a suitable model along with a consideration of model uncertainty (Box 9.4), before it eventually is applied to assess low flow and drought in the region of interest.

Box 9.4 Uncertainty aspects in process-based models

There are many causes of uncertainty in a (socio-)hydrological modelling study. Recognising, assessing and communicating uncertainty are crucial to provide reliable information to users (e.g., stakeholders, water managers, politicians) (Section 13.5). Needless to say, that by definition all (socio-)hydrological models, including their outputs, are associated with uncertainties. Uncertainties that originate from different sources: (a) model structure, (b) model parameters, and (c) input data, either initial or boundary conditions, calibration and validation data, including measurements, derived data, and scaling uncertainties (Section 4.2.6).

The three hydrological models (HVB, PCR-GLOBWB and SIMGRO) described in detail in this chapter (Fig. 9.1) represent key differences in model structure (first source of uncertainty). This includes, for example, whether and not they divide the model domain into spatial distinct model units. Some processes are missing in some models, such as snow accumulation and melting in SIMGRO, and distributed groundwater flow in HBV, because the models were not developed for these purposes. Complexity in model structure can be viewed as the number of processes explicitly included and the number of interactions and feedbacks incorporated. Confidence is not necessarily higher in simulations from a complex model compared to a simple one (Baartman et al., 2020). Furthermore, when selecting a model it is important to be aware that different model versions, with different level of complexity and processes represented, exist. For example, the standard PCR-GLOBWB has an integral nature (nGWfl, Section 9.4.2), but a more recent version simulates lateral saturated groundwater flow (differential nature, GWfl); application of the GWfl version was found to have a large effect on the simulated worldwide impact of groundwater pumping (De Graaf and Stahl, 2022). Differences in results between models with and without simulation of lateral saturated groundwater flow (GWfl versus nGWfl) can

Box 9.4 Uncertainty aspects in process-based models—cont'd

be interpreted as a source of model structure uncertainty. Large-scale models are traditionally setup with a low spatial resolution, which allows to get a quick overview of the global or continental situation, but makes them less suitable for catchment-scale analysis and management tools. However, large-scale models are becoming increasingly adapted to higher spatial resolutions, commonly referred to as hyper-resolution models (Bierkens, 2015; Hoch et al., 2023). Large-scale models often perform less well (on low flow or hydrological drought) in regions with large storages (e.g., groundwater, lakes) and in seasonal snow climates due to uncertainties in the parametrisation of storage and related response functions as well as cold climate processes (Stahl et al., 2012; Van Loon et al., 2012). The three types of socio-hydrological modelling approaches, exemplified by selected model applications (Sections 9.5.2, 9.5.3 and 9.5.4), have very different model structures. For example, model structures of coupled-component modelling are similar to hydrological model structures, whereas the model structure of agent-based modelling has a completely different starting point, that is, behavioural theory. Uncertainties will be associated with the choice of one the different model structures.

The second source of uncertainty in (socio-)hydrological modelling is parameter uncertainty. Generally, more complex models (more processes involved, distributed versus lumped) require more parameters, which imposes challenges, although some parameters can be effectively upscaled using observations rather than calibrated values (Section 9.2.3). When calibrating a model, one should consider equifinality, that is, there exists no global optimum set of parameters, but many potential parameter sets that produce equally good hydrological performance. Furthermore, validation merely on river flow does not imply that internal fluxes (e.g., actual evapotranspiration) or states (e.g., soil moisture, groundwater) are equally well simulated (Bouaziz et al., 2020).

The third source of uncertainty are the input data, which means for most (socio-)hydrological models time series of observed (or estimated observed) meteorological data used as forcing and observed hydrological data for calibration and validation of the models (Fig. 9.1, Section 9.2). Lumped hydrological models require river flow data, and in case of distributed models additional river flow data from sub-catchments that may be simultaneously used to calibrate the model (Engeland et al., 2001). Catchment models with a differential nature (Section 9.4.3) require time series of groundwater hydraulic heads to calibrate and define aquifer boundary conditions and defining these may be challenging in some cases. Moreover, these catchment models, like other models with a differential nature, need spatially distributed groundwater hydraulic heads (i.e., from groundwater contour maps) to specify initial conditions.

The use of multi-model ensembles (representing different model structures, parameter sets and input data) has been advocated as the best way to quantify uncertainty of process-based models (Box 11.2). This approach addresses the so-called aleatory uncertainty, that is, the uncertainty related to random variability. Probabilistic methods are helpful to consider uncertainty related to randomness. So, aleatory uncertainty can be handled, but how to deal with lack of knowledge, that is, epistemic uncertainty (fourth source of uncertainty), is a real challenge. Even though hydrological knowledge is far from perfect (e.g., Merz and Thieken, 2005), dealing with epistemic uncertainty is in particular relevant for socio-hydrology, as social dynamics and their interplay with hydrological changes are basically unknown. Knowledge in the behaviour of human-water systems is generally lacking, namely: (a) known unknowns (knowledge one knows that it does not exist), and (b) unknown unknowns (knowledge one even does not know that is missed); and knowledge can be erroneous (knowledge one thinks is known, but actually is unknown) (Di Baldassarre et al., 2016). Decision-makers should be made aware of epistemic uncertainty in process-based models and to be prepared that so-called 'black swans' (unpredicted events with an extremely high impact) may appear.

9.7 Summary

The main principle of process-based models is that they build upon (socio-)hydrological knowledge to describe one or more processes. The role of process-based models (socio-)hydrological models in the whole modelling framework is elaborated, starting with different types of forcing datasets and ending with the identification of (socio-)hydrological drought. Generic aspects of model calibration and validation are given, such as goodness-of-fit criteria, different ways to estimate model parameters and to implement split-sampling.

(Spatially) lumped, semi-distributed and (spatially) distributed (socio-)hydrological models are distinguished based on how they represent the model space (spatial scale). Lumped models represent the model domain (e.g., catchment) as one column and have areal-averaged input and output. Semi-distributed models consist of several columns (spatial units) that permit the user to consider, for example, different land use, elevation, and soil characteristics, in the hydrological analysis. The columns in semi-distributed models, however, do not have a specific location in space in the model setup. In (fully) distributed models, the columns do have a specific location, which allows, for example, routing the simulated runoff from one column to the next, eventually accumulated at the outlet of the catchment, which can make them more suited for spatial drought analysis, irrespectly of catchment scale. Most distributed models do not simulate saturated lateral groundwater flow (integral models, nGWfl). Distributed models that allow the simulation of lateral groundwater are of a differential nature (GWfl), which allows to investigate specific groundwater-drought related issues (e.g., impact of groundwater abstraction on a nearby nature reserve). HBV, PCR-GLOBWB and SIMGRO have been selected as example hydrological models to explain lumped catchment models, large-scale distributed models and catchment distributed models, respectively. The models are applied to show the influence of human interventions on time series of river flow and groundwater levels.

Process-based socio-hydrological models can similar to hydrological models be lumped or distributed. Three socio-hydrological modelling approaches are described (coupled-component, system-dynamics and agent-based modelling). The approaches are developed to describe long-term interactions between hydrology and human actions, and hydrological processes are usually described in less detail. Agent-based modelling can be classified as a bottom-up approach, that is, starting point is behaviour of individuals, whereas coupled-component and system-dynamics modelling can be characterised as top-down approaches that investigates the system with a more generic description of human behaviour. Three types of socio-hydrological approaches are introduced along with examples, that is, coupled-component models, system-dynamics models and agent-based models. The examples include drought management and groundwater abstraction, the collapse of the Maya society, reservoir operation policy and adaptation behaviour of east African farmers.

The chapter concludes with guidance on how to select an adequate process-based model to study low flow or hydrological drought, particularly addressing model complexity and sources of uncertainties.

9.8 Further reading

Beven, K.J., 2012. Rainfall-runoff modelling : the primer. Second ed., John Wiley & Sons, Chichester, UK. https://onlinelibrary.wiley.com/doi/book/10.1002/9781119951001.

Bierkens, M.F.P., 2015. Global hydrology 2015: State, trends, and directions. Water Resour. Res. 51, 4923−4947. https://doi.org/10.1002/2015WR017173.

Blair, P., Buytaert, W., 2016. Socio-hydrological modelling: a review asking "why, what and how?". Hydrol. Earth Syst. Sc. 20(1), 443−478. https://doi.org/10.5194/hess-20-443-2016.

Hrachowitz, M., Clark, M.P., 2017. HESS Opinions: The complementary merits of competing modelling philosophies in hydrology. Hydrol. Earth Syst. Sc. 21, 3953−3973. https://doi.org/10.5194/hess-21-3953-2017.

Seibert, J., Bergström, S., 2022. A retrospective on hydrological catchment modelling based on half a century with the HBV model. Hydrol. Earth Syst. Sc. 26, 1371−1388. https://doi.org/10.5194/hess-26-1371-2022.

References

Addor, N., Melsen, L.A., 2018. Legacy, rather than adequacy, drives the selection of hydrological models. Water Resour. Res. 55, 378–390. https://doi.org/10.1029/2018WR022958.

Akter, S., Grafton, R.Q., Merritt, W.S., 2014. Integrated hydro-ecological and economic modeling of environmental flows: macquarie Marshes. Agric. Water Manage. 145, 98–109. https://doi.org/10.1016/j.agwat.2013.12.005.

Alcamo, J., Döll, P., Henrichs, T., Kaspar, F., Lehner, B., Rösch, T., Siebert, S., 2003. Development and testing of the WaterGAP 2 global model of water use and availability. Hydrolog. Sci. J. 48 (3), 317–333. https://doi.org/10.1623/hysj.48.3.317.45290.

Arnell, N.W., 2004. Climate change and global water resources: SRES emissions and socio economic scenarios. Global Environ. Change 14 (1), 31–52. https://doi.org/10.1016/j.gloenvcha.2003.10.006.

Astagneau, P., Thirel, G., Delaigue, O., 2020. Hydrology modelling R packages: codes for simulating streamflow using one parameter set. https://doi.org/10.15454/3PPKCL.

Astagneau, P.C., Thirel, G., Delaigue, O., Guillaume, J.H.A., Parajka, J., Brauer, C.C., Viglione, A., Buytaert, W., Beven, K.J., 2021. Technical note: hydrology modelling R packages — a unified analysis of models and practicalities from a user perspective. Hydrol. Earth Syst. Sci. 25, 3937–3973. https://doi.org/10.5194/hess-25-3937-2021.

Baartman, J.E.M., Melsen, L.A., Moore, D., Vander Ploeg, M.J., 2020. On the complexity of model complexity: viewpoints across the geosciences. Catena 186, 104261. https://doi.org/10.1016/j.catena.2019.104261.

Barreteau, O., Sauquet, E., Riaux, J., Gailliard, N., Barbier, R., 2014. Agent based simulation of drought management in practice. In: Kamiński, B., Koloch, G. (Eds.), Advances in Social Simulation, Advances in Intelligent Systems and Computing, vol 229. Springer, Berlin, Heidelberg, pp. 237–248. https://doi.org/10.1007/978-3-642-39829-2_21.

Barthel, R., Reichenau, T.G., Krimly, T., Dabbert, S., Schneider, K., Mauser, W., 2012. Integrated modeling of global change impacts on agriculture and groundwater resources. Water Resour. Manag. 26 (7), 1929–1951. https://doi.org/10.1007/s11269-012-0001-9.

Beck, H.E., van Dijk, A.I.J.M., de Roo, A., Miralles, D.G., McVicar, T.R., Schellekens, J., Bruijnzeel, L.A., 2016. Global-scale regionalization of hydrologic model parameters. Water Resour. Res. 52, 3599–3622. https://doi.org/10.1002/2015WR018247.

Bergström, S., 1992. The HBV Model: Its Structure and Applications. Swedish Meteorological and Hydrological Institute (SMHI), Hydrology, Norrköping. https://www.smhi.se/polopoly_fs/1.83592!/Menu/general/extGroup/attachmentColHold/mainCol1/file/RH_4.pdf.

Beven, K.J., 2012. Rainfall-runoff Modelling: The Primer, Second ed. John Wiley & Sons, Chichester, UK https://onlinelibrary.wiley.com/doi/book/10.1002/9781119951001.

Bierkens, M.F.P., 2015. Global hydrology 2015: state, trends, and directions. Water Resour. Res. 51, 4923–4947. https://doi.org/10.1002/2015WR017173.

Blair, P., Buytaert, W., 2016. Socio-hydrological modelling: a review asking "why, what and how?". Hydrol. Earth Syst. Sci. 20 (1), 443–478. https://doi.org/10.5194/hess-20-443-2016.

Bouaziz, L.J.E., Thirel, G., De Boer-Euser, T., Melsen, L.A., Buitink, J., Brauer, C.C., De Niel, J., Moustakas, S., Willems, P., Grelier, B., Drogue, G., Fenicia, F., Nossent, J., Pereira, F., Sprokkereef, E., Stam, J., Dewals, B.J., Weerts, A.H., Savenije, H.H.G., Hrachowitz, M., 2020. Behind the scenes of streamflow model performance. Hydrol. Earth Syst. Sci. 25 (2), 1069–1095. https://doi.org/10.5194/hess-2020-176.

Boussetta, S., Balsamo, G., Beljaars, A., Agusti-Panareda, A., Calvet, J.-C., Jacobs, C., van den Hurk, B., Viterbo, P., Lafont, S., Dutra, E., Jarlan, L., Balzarolo, M., Papale, D., van der Werf, G., 2012. Natural Land Carbon Dioxide Exchanges in the ECMWF Integrated Forecasting System: Implementation and Offline Validation. ECMWF, Reading, UK. Technical Memorandum 675. https://www.ecmwf.int/sites/default/files/elibrary/2012/8338-natural-carbon-dioxide-exchanges-ecmwf-integrated-forecasting-system-implementation-and-offline.pdf.

Brauer, C.C., Torfs, P.J.J.F., Teuling, A.J., Uijlenhoet, R., 2014. The Wageningen Lowland Runoff Simulator (WALRUS): application to the Hupsel Brook catchment and the Cabauw polder. Hydrol. Earth Syst. Sci. 18, 4007−4028. https://doi.org/10.5194/hess-18-4007-2014.

Burek, P., Van der Knijff, J., De Roo, A., 2013. LISFLOOD Distributed Water Balance and Flood Simulation Model. Revised User Manual, Reference Report, JRC78917. Joint Research Centre of the European Commission, Ispra, Italy. https://doi.org/10.2788/24982.

Castilla-Rho, J.C., Mariethoz, G., Rojas, R., Andersen, M.S., Kelly, B.F.J., 2015. An agent-based platform for simulating complex human-aquifer interactions in managed groundwater systems. Environ. Model. Softw. 73, 305−323. https://doi.org/10.1016/j.envsoft.2015.08.018.

Clark, M.P., Slater, A.G., Rupp, D.E., Woods, R.A., Vrugt, J.A., Gupta, H.V., Wagener, T., Hay, L.E., 2008. Framework for Understanding Structural Errors (FUSE): a modular framework to diagnose differences between hydrological models. Water Resour. Res. 44, W00B02. https://doi.org/10.1029/2007WR006735.

Clark, M.P., Nijssen, B., Lundquist, J.D., Kavetski, D., Rupp, D.E., Woods, R.A., Freer, J.E., Gutmann, E.D., Wood, A.W., Brekke, L.D., Arnold, J.R., Gochis, D.J., Rasmussen, R.M., 2015. A unified approach for process-based hydrologic modeling: 1. Modeling concept. Water Resour. Res. 51, 2498−2514. https://doi.org/10.1002/2015WR017198.

Compo, G.P., Whitaker, J.S., Sardeshmukh, P.D., Matsui, N., Allan, R.J., Yin, X., Gleason Jr., B.E., Vose, R.S., Rutledge, G., Bessemoulin, P., Brönnimann, S., Brunet, M., Crouthamel, R.I., Grant, A.N., Groisman, P.Y., Jones, P.D., Kruk, M.C., Kruger, A.C., Marshall, G.J., Maugeri, M., Mok, H.Y., Nordli, Ø., Ross, T.F., Trigo, R.M., Wang, X.L., Woodruff, S.D., Worley, S.J., 2011. The twentieth century reanalysis project. Q. J. R. Meteorol. Soc. 137, 1−28. https://doi.org/10.1002/qj.776.

Cornes, R., Van der Schrier, G., Van den Besselaar, E.J.M., Jones, P.D., 2018. An ensemble version of the E-OBS temperature and precipitation datasets. J. Geophys. Res. Atmos. 123 (17), 9391−9409. https://doi.org/10.1029/2017JD028200.

Cucchi, M., Weedon, G.P., Amici, A., Bellouin, N., Lange, S., Müller Schmied, H., Hersbach, H., Buontempo, C., 2020. WFDE5: bias adjusted ERA5 reanalysis data for impact studies. Earth Syst. Sci. Data 12, 2097−2120. https://doi.org/10.5194/essd-12-2097-2020.

De Graaf, I.E.M., Sutanudjaja, E.H., Van Beek, L.P.H., Bierkens, M.F.P., 2015. A high-resolution global-scale groundwater model. Hydrol. Earth Syst. Sci. 19 (2), 823−837. https://doi.org/10.5194/hess-19-823-2015.

De Graaf, I.E.M., Stahl, K., 2022. A model comparison assessing the importance of lateral groundwater flows at the global scale. Environ. Res. Lett. 17, 044020. https://doi.org/10.1088/1748-9326/ac50d2.

De Lange, W.J., Prinsen, G.F., Hoogewoud, J.C., Veldhuizen, A.A., Verkaik, J., Oude Essink, G.H.P., Van Walsum, P.E.V., Delsman, J.R., Hunink, J.C., Massop, H.T.L., Kroon, T., 2014. An operational, multi-scale, multi-model system for consensus-based, integrated water management and policy analysis: The Netherlands Hydrological Instrument. Environ. Model. Softw. 59, 98−108. https://doi.org/10.1016/j.envsoft.2014.05.009.

Dee, D.P., Uppalaa, S.M., Simmons, A.J., Berrisford, P., Polia, P., Kobayashib, S., Andrae, U., Balmasedaa, M.A., Balsamo, G., Bauera, P., Bechtold, P., Beljaars, A.C.M., van de Berg, L., Bidlot, J., Bormann, N., Delsol, C., Dragani, R., Fuentes, M., Geer, A.J., Haimberger, L., Healy, S.B., Hersbach, H., Hólm, E.V., Isaksen, L., Källberg, P., Köhler, M., Matricardi, M., McNally, A.P., Monge-Sanz, B.M., Morcrette, J.-J., Park, B.-K., Peubey, C., de Rosnay, P., Tavolato, C., Thépaut, J.-N., Vitart, F., 2011. The ERA-Interim reanalysis: configuration and performance of the data assimilation system. Q. J. R. Meteorol. Soc. 137, 553−597. https://doi.org/10.1002/qj.828.

Di Baldassarre, G., Viglione, A., Carr, G., Kuil, L., Salinas, J.L., Blöschl, G., 2013. Socio-hydrology: conceptualising human-flood interactions. Hydrol. Earth Syst. Sci. 17, 3295−3303. https://doi.org/10.5194/hess-17-3295-2013.

Di Baldassarre, G., Brandimarte, L., Beven, K., 2016. The seventh facet of uncertainty: wrong assumptions, unknowns and surprises in the dynamics of human−water systems. Hydrolog. Sci. J. 61 (9), 1748−1758. https://doi.org/10.1080/02626667.2015.1091460.

Di Baldassarre, G., Sivapalan, M., Rusca, M., Cudennec, C., Garcia, M., Kreibich, H., Konar, M., Mondino, E., Mård, J., Pande, S., Sanderson, M.R., Tian, F., Viglione, A., Wei, J., Wei, Y., Yu, D.J., Srinivasan, V.,

Blöschl, G., 2019. Sociohydrology: scientific challenges in addressing the sustainable development goals. Water Resour. Res. 55, 6327−6355. https://doi.org/10.1029/2018WR023901.

Engeland, K., Gottschalk, L., Tallaksen, L.M., 2001. Estimation of regional parameters in a macro scale hydrological model. Nord. Hydrol 32 (3), 161−180. https://doi.org/10.2166/NH.2001.0010.

Essery, R.L.H., Best, M.J., Betts, R.A., Cox, P.M., Taylor, C.M., 2003. Explicit representation of subgrid heterogeneity in a GCM land surface scheme. J. Hydrometeor. 4 (3), 530−543. https://doi.org/10.1175/1525-7541(2003)004<0530:EROSHI>2.0.CO;2.

Euser, T., Winsemius, H.C., Hrachowitz, M., Fenicia, F., Uhlenbrook, S., Savenije, H.H.G., 2013. A framework to assess the realism of model structures using hydrological signatures. Hydrol. Earth Syst. Sci. 17, 1893−1912. https://doi.org/10.5194/hess-17-1893-2013.

Falter, D., Schröter, K., Dung, N.V., Vorogushyn, S., Kreibich, H., Hundecha, Y., Apel, H., Merz, B., 2015. Spatially coherent flood risk assessment based on long-term continuous simulation with a coupled model chain. J. Hydrol. 524, 182−193. https://doi.org/10.1016/j.jhydrol.2015.02.021.

Fatichi, S., Vivoni, E.R., Ogden, F.L., Ivanov, V.Y., Mirus, B., Gochis, D., Downer, C.W., Camporese, M., Davison, J.H., Ebel, B., Jones, N., Kim, J., Mascaro, G., Niswonger, R., Restrepo, P., Rigon, R., Shen, C., Sulis, M., Tarboton, D., 2016. An overview of current applications, challenges, and future trends in distributed process-based models in hydrology. J. Hydrol. 537, 45−60. https://doi.org/10.1016/j.jhydrol.2016.03.026.

Fenicia, F., Kavetski, D., Savenije, H.H.G., Clark, M.P., Schoups, G., Pfister, L., Freer, J., 2014. Catchment properties, function, and conceptual model representation: is there a correspondence? Hydrol. Process. 2 (4), 2451−2467. https://doi.org/10.1002/hyp.9726.

Feyen, L., Dankers, R., 2009. Impact of global warming on streamflow drought in Europe. J. Geophys. Res. Atmos. 114, D17. https://doi.org/10.1029/2008JD011438.

Garcia, M., Portney, K., Islam, S., 2016. A question driven socio-hydrological modeling process. Hydrol. Earth Syst. Sci. 20, 73−92. https://doi.org/10.5194/hess-20-73-2016.

Garcia, F., Folton, N., Oudin, L., 2017. Which objective function to calibrate rainfall−runoff models for low-flow index simulations? Hydrolog. Sci. J. 62 (7), 1149−1166. https://doi.org/10.1080/02626667.2017.1308511.

Gelaro, R., McCarty, W., Suárez, M.J., Todling, R., Molod, A., Takacs, L., Randles, C.A., Darmenov, A., Bosilovich, M.G., Reichle, R., Wargan, K., Coy, L., Cullather, R., Draper, C., Akella, S., Buchard, V., Conaty, A., Da Silva, A.M., Gu, W., Kim, G.-K., Koster, R., Lucchesi, R., Merkova, D., Nielsen, J.E., Partyka, G., Pawson, S., Putman, W., Rienecker, M., Schubert, S.D., Sienkiewicz, M., Zhao, B., 2017. The modern-era retrospective analysis for research and applications, version 2 (MERRA-2). J. Climate 30 (14), 5419−5454. https://doi.org/10.1175/JCLI-D-16-0758.1.

Giuliani, M., Li, Y., Castelletti, A., Gandolfi, C., 2016. A coupled human-natural systems analysis of irrigated agriculture under changing climate. Water Resour. Res. 52 (9), 6928−6947. https://doi.org/10.1002/2016WR019363.

Gosling, S.N., Arnell, N.W., 2010. Simulating current global river runoff with a global hydrological model: model revisions, validation and sensitivity analysis. Hydrol. Process. 25 (7), 1129−1145. https://doi.org/10.1002/hyp.7727.

Gudmundsson, L., Tallaksen, L.M., Stahl, K., Clark, D.B., Dumont, E., Hagemann, S., Bertrand, N., Gerten, D., Heinke, J., Hanasaki, N., Voss, F., Koirala, S., 2012. Comparing large-scale hydrological model simulations to observed runoff percentiles in Europe. J. Hydrometeorol. 13 (2), 604−620. https://doi.org/10.1175/JHM-D-11-083.1.

Guimberteau, M., Zhu, D., Maignan, F., Huang, Y., Yue, C., Dantec-Nédélec, S., Ottlé, C., Jornet-Puig, A., Bastos, A., Laurent, P., Goll, D., Bowring, S., Chang, J., Guenet, B., Tifafi, M., Peng, S., Krinner, G., Ducharne, A., Wang, F., Wang, T., Wang, X., Wang, Y., Yin, Z., Lauerwald, R., Joetzjer, E., Qiu, C., Kim, H., Ciais, P., 2018. ORCHIDEE-MICT (v8.4.1), a land surface model for the high latitudes: model description and validation. Geosci. Model Dev. 11, 121−163. https://doi.org/10.5194/gmd-11-121-2018.

Gupta, H.V., Kling, H., Yilmaz, K.K., Martinez, G.F., 2009. Decomposition of the mean squared error and NSE performance criteria: implications for improving hydrological modelling. J. Hydrol. 377, 80−91. https://doi.org/10.1016/j.jhydrol.2009.08.003.

Haddeland, I., Clark, D.B., Franssen, W., Ludwig, F., Voss, F., Arnell, N.W., Bertrand, N., Best, M., Folwell, S., Gerten, D., Gomes, S., Gosling, S.N., Hagemann, S., Hanasaki, N., Harding, R., Heinke, J., Kabat, P., Koirala, S., Oki, T., Polcher, J., Stacke, T., Viterbo, P., Weedon, G.P., Yeh, P., 2011. Multi-model estimate of the global terrestrial water balance: setup and first results. J. Hydrometeorol. 12, 869−884. https://doi.org/10.1175/2011JHM1324.1.

Hagemann, S., Gates, L.D., 2003. Improving a subgrid runoff parameterization scheme for climate models by the use of high resolution data derived from satellite observations. Clim. Dynam. 21, 349−359. https://doi.org/10.1007/s00382-003-0349-x.

Hamon, W.R., 1961. Estimating potential evapotranspiration. J. Hydraul. Eng. 87 (3), 107−120. https://doi.org/10.1061/JYCEAJ.0000599.

Hanasaki, N., Kanae, S., Oki, T., Masuda, K., Motoya, K., Shirakawa, N., Shen, Y., Tanaka, K., 2008. An integrated model for the assessment of global water resources − Part 1: model description and input meteorological forcing. Hydrol. Earth Syst. Sci. 12, 1007−1025. https://doi.org/10.5194/hess-12-1007-2008.

Hanel, M., Rakovec, O., Markonis, Y., Máca, P., Samaniego, L., Kyselý, J., Kumar, R., 2018. Revisiting the recent European droughts from a long-term perspective. Sci. Rep. 8, 9499. https://doi.org/10.1038/s41598-018-27464-4.

Hersbach, H., Bell, B., Berrisford, P., Hirahara, S., Horányi, A., Muñoz-Sabater, J., Nicolas, J., Peubey, C., Radu, R., Schepers, D., Simmons, A., Soci, C., Abdalla, S., Abellan, X., Balsamo, G., Bechtold, P., Biavati, G., Bidlot, J., Bonavita, M., De Chiara, G., Dahlgren, P., Dee, D., Diamantakis, M., Dragani, R., Flemming, J., Forbes, R., Fuentes, M., Geer, A., Haimberger, L., Healy, S., Hogan, R.J., Hólm, E., Janisková, M., Keeley, S., Laloyaux, P., Lopez, P., Lupu, C., Radnoti, G., de Rosnay, P., Rozum, I., Vamborg, F., Villaume, S., Thépaut, J.-N., 2020. The ERA5 global reanalysis. Q. J. R. Meteorol. Soc. 146, 1999−2049. https://doi.org/10.1002/qj.3803.

Hoch, J.M., Sutanudjaja, E.H., Wanders, N., van Beek, R.L.P.H., Bierkens, M.F.P., 2023. Hyper-resolution PCR-GLOBWB: opportunities and challenges of refining model spatial resolution to 1 km over the European continent. Hydrol. Earth Syst. Sci. 27, 1383−1401. https://doi.org/10.5194/hess-27-1383-2023.

Hrachowitz, M., Clark, M.P., 2017. HESS Opinions: the complementary merits of competing modelling philosophies in hydrology. Hydrol. Earth Syst. Sci. 21, 3953−3973. https://doi.org/10.5194/hess-21-3953-2017.

Kampf, S.K., Burges, S.J., 2007. A framework for classifying and comparing distributed hillslope and catchment hydrologic models. Water Resour. Res. 43, W05423. https://doi.org/10.1029/2006WR005370.

Klemeš, V., 1986. Operational testing of hydrological simulation models. Hydrolog. Sci. J. 31 (1), 13−24. https://doi.org/10.1080/02626668609491024.

Kobayashi, S., Ota, Y., Harada, Y., Ebita, A., Moriya, M., Onoda, H., Onogi, K., Kamahori, H., Kobayashi, C., Endo, H., Miyaoka, K., Takahashi, K., 2015. The JRA-55 Reanalysis: general specifications and basic characteristics. J. Meteorol. Soc. Jpn. Ser. II 93 (1), 5−48. https://doi.org/10.2151/jmsj.2015-001.

Koirala, S., 2010. Explicit Representation of Groundwater Process in a Global-Scale Land Surface Model to Improve Hydrological Predictions. PhD thesis Civil Engineering. The University of Tokyo, Japan.

Kroes, J.G., Van Dam, J.C., Bartholomeus, R.P., Groenendijk, P., Heinen, M., Hendriks, R.F.A., Mulder, H.M., Supit, I., Van Walsum, P.E.V., 2017. SWAP Version 4; Theory Description and User Manual. Wageningen, Wageningen Environmental Research, the Netherlands. Report 2780. http://library.wur.nl/WebQuery/wurpubs/fulltext/416321.

Kuil, L., Carr, G., Viglione, A., Prskawetz, A., Blöschl, G., 2016. Conceptualizing socio-hydrological drought processes: the case of the Maya collapse. Water Resour. Res. 52, 6222−6242. https://doi.org/10.1002/2015WR018298.

Kuil, L., Evans, T., McCord, P., Salinas, J., Bloschl, G., 2018. Exploring the influence of smallholders' perceptions regarding water availability on crop choice and water allocation through socio-hydrological modeling. Water Resour. Res. 54 (4), 2580−2604. https://doi.org/10.1002/2017WR021420.

Lehner, B., Reidy Liermann, C., Revenga, C., Vörösmarty, C., Fekete, B., Crouzet, P., Döll, P., Endejan, M., Frenken, K., Magome, J., Nilsson, C., Robertson, J.C., Rodel, R., Sindorf, N., Wisser, D., 2011. High-resolution mapping of the world's reservoirs and dams for sustainable river-flow management. Front. Ecol. Environ. 9 (9), 494−502. https://doi.org/10.1890/100125.

Liang, X., Wood, E.F., Lettenmaier, D.P., 1996. Surface soil moisture parameterization of the VIC-2L model: evaluation and modification. Global Planet. Change 13, 195−206. https://doi.org/10.1016/0921-8181(95)00046-1.

Mai, J., 2023. Ten strategies towards successful calibration of environmental models. J. of Hydrology 620, 129414. https://doi.org/10.1016/j.jhydrol.2023.129414.

Maneta, M.P., Torres, M.D.O., Wallender, W.W., Vosti, S., Howitt, R., Rodrigues, L., Bassoi, L.H., Panday, S., 2009. A spatially distributed hydroeconomic model to assess the effects of drought on land use, farm profits, and agricultural employment. Water Resour. Res. 45 (11), W11412. https://doi.org/10.1029/2008WR007534.

Matthews, R.B., Gilbert, N.G., Roach, A., Polhill, J.G., Gott, N.M., 2007. Agent-based land-use models: a review of applications. Landsc. Ecol. 22, 1447−1459. https://doi.org/10.1007/s10980-007-9135-1.

McNider, R.T., Handyside, C., Doty, K., Ellenburg, W.L., Cruise, J.F., Christy, J.R., Moss, D., Sharda, V., Hoogenboom, G., Caldwell, P., 2015. An integrated crop and hydrologic modeling system to estimate hydrologic impacts of crop irrigation demands. Environ. Model. Softw. 72, 341−355. https://doi.org/10.1016/j.envsoft.2014.10.009.

Meigh, J.R., McKenzie, A.A., Sene, K.J., 1999. A grid-based approach to water scarcity estimates for eastern and southern Africa. Water Resour. Manag. 13, 85−115. https://doi.org/10.1023/A:100802570371.

Merz, B., Thieken, A.H., 2005. Separating natural and epistemic uncertainty in flood frequency analysis. J. Hydrol. 309, 114−132. https://doi.org/10.1016/j.jhydrol.2004.11.015.

Meza, I., Siebert, S., Döll, P., Kusche, J., Herbert, C., Eyshi Rezaei, E., Nouri, H., Gerdener, H., Popat, E., Frischen, J., Naumann, G., Vogt, J.V., Walz, Y., Sebesvari, Z., Hagenlocher, M., 2020. Global-scale drought risk assessment for agricultural systems. Nat. Hazards Earth Syst. Sci. 20, 695−712. https://doi.org/10.5194/nhess-20-695-2020.

Newman, A.J., Clark, M.P., Craig, J., Nijssen, B., Wood, A., Gutmann, E., Mizukami, N., Brekke, L., Arnold, J.R., 2015. Gridded ensemble precipitation and temperature estimates for the contiguous United States. J. Hydrometeorol. 16 (6), 2481−2500. https://doi.org/10.1175/JHM-D-15-0026.1.

Niu, G.-Y., Yang, Z.-L., Mitchell, K.E., Chen, F., Ek, M.B., Barlage, M., Kumar, A., Manning, K., Niyogi, D., Rosero, E., Tewari, M., Xia, Y., 2011. The community Noah land surface model with multi parameterization options (Noah-MP): 1. Model description and evaluation with local-scale measurements. J. Geophys. Res. Atmos. 116, D12109. https://doi.org/10.1029/2010JD015139.

Prudhomme, C., Giuntoli, I., Robinson, E.L., Clark, D.B., Arnell, N.W., Dankers, R., Fekete, B.M., Franssen, W., Gerten, D., Gosling, S.N., Hagemann, S., Hannah, D.M., Kim, H., Masaki, Y., Satoh, Y., Stacke, T., Wada, Y., Wisser, D., 2014. Hydrological droughts in the 21st century, hotspots and uncertainties from a global multimodel ensemble experiment. Proc. Natl. Acad. Sci. U. S. A. 111 (9), 3262−3267. https://doi.org/10.1073/pnas.1222473110.

Querner, E.P., 1988. Description of a regional groundwater flow model SIMGRO and some applications. Agric. Water Manage. 14, 209−218. https://doi.org/10.1016/0378-3774(88)90075-3.

Querner, E.P., Van Lanen, H.A.J., 2001. Impact assessment of drought mitigation measures in two adjacent Dutch basins using simulation modelling. J. Hydrol. 252, 51−64. https://doi.org/10.1016/S0022-1694(01)00452-8.

Rost, S., Gerten, D., Bondeau, A., Lucht, W., Rohwer, J., Schaphoff, S., 2008. Agricultural green and blue water consumption and its influence on the global water system. Water Resour. Res. 44, W09405. https://doi.org/10.1029/2007WR006331.

Sælthun, N.R., 1996. The "Nordic" HBV model. Description and documentation of the model version developed for the project Climate Change and Energy Production. NVE Report No. 7. The Norwegian Water Resources and Energy Administration, Norway. https://www.osti.gov/etdeweb/servlets/purl/515690.

Samaniego, L., Thober, S., Wanders, N., Pan, M., Rakovec, O., Sheffield, J., Wood, E.F., Prudhomme, C., Rees, G., Houghton-Carr, H., Fry, M., Smith, K., Watts, G., Hisdal, H., Estrela, T., 2019. Hydrological forecasts and projections for improved decision-making in the water sector in Europe. Bull. Am. Meteorol. Soc. 2451−2472. https://doi.org/10.1175/BAMS-D-17-0274.1.

Seibert, J., 1999. Regionalisation of parameters for a conceptual rainfall runoff model. Agric. Forest Meteorol. 98, 279−293. https://doi.org/10.1016/S0168-1923(99)00105-7.

Seibert, J., 2000. Multi-criteria calibration of a conceptual runoff model using a genetic algorithm. Hydrol. Earth Syst. Sci. 4 (2), 215−224. https://doi.org/10.5194/hess-4-215-2000.

Seibert, J., 2005. HBV Light version 2, User's Manual. https://web.archive.org/web/20150603172034/http://www.geo.uzh.ch/fileadmin/files/content/abteilungen/h2k/Docs_download/HBV_manual_2005.pdf.

Seibert, J., Vis, M., 2012. Teaching hydrological modeling with a user-friendly catchment-runoff-model software package. Hydrol. Earth Syst. Sci. 16, 3315−3325. https://doi.org/10.5194/hess-16-3315-2012.

Seibert, J., Bergström, S., 2022. A retrospective on hydrological catchment modelling based on half a century with the HBV model. Hydrol. Earth Syst. Sci. 26, 1371−1388. https://doi.org/10.5194/hess-26-1371-2022.

Sheffield, J., Wood, E.F., 2008. Global trends and variability in soil moisture and drought characteristics, 1950−2000, from observation-driven simulations of the terrestrial hydrologic cycle. J. Climate 21, 432−458. https://doi.org/10.1175/2007JCLI1822.1.

Shen, H., Tolson, B.A., Mai, J., 2022. Time to update the split sample approach in hydrological model calibration. Water Resour. Res. 58, e2021WR031523. https://doi.org/10.1029/2021WR031523.

Sivapalan, M., Savenije, H.H.G., Blöschl, G., 2012. Socio-hydrology: a new science of people and water. Hydrol. Process. 26, 1270−1276. https://doi.org/10.1002/hyp.8426.

Srinivasan, V., Sanderson, M., Garcia, M., Konar, M., Blöschl, G., Sivapalan, M., 2017. Prediction in a socio-hydrological world. Hydrolog. Sci. J. 62 (3), 338−345. https://doi.org/10.1080/02626667.2016.1253844.

Stahl, K., Moore, R.D., Shea, J.M., Hutchinson, D., Cannon, A.J., 2008. Coupled modelling of glacier and streamflow response to future climate scenarios. Water Resour. Res. 44, W02422. https://doi.org/10.1029/2007WR005956.

Stahl, K., Tallaksen, L.M., Hannaford, J., Van Lanen, H.A.J., 2012. Filling the white space on maps of European runoff trends: estimates from a multi-model ensemble. Hydrol. Earth Syst. Sci. 16, 2035−2047. https://doi.org/10.5194/hess-16-2035-2012.

Staudinger, M., Stahl, K., Seibert, J., Clark, M.P., Tallaksen, L.M., 2011. Comparison of hydrological model structures based on recession and low flow simulations. Hydrol. Earth Syst. Sci. 15, 3447−3459. https://doi.org/10.5194/hess-15-3447-2011.

Sutanudjaja, E.H., van Beek, L.P.H., De Jong, S.M., Van Geer, F.C., Bierkens, M.F.P., 2014. Calibrating a large-extent high-resolution coupled groundwater-land surface model using soil moisture and discharge data. Water Resour. Res. 50, 687−705. https://doi.org/10.1002/2013WR013807.

Sutanudjaja, E.H., Van Beek, R., Wanders, N., Wada, Y., Bosmans, J.H.C., Drost, N., Van der Ent, R.J., De Graaf, I.E.M., Hoch, J.M., De Jong, K., Karssenberg, D., López López, P., Peßenteiner, S., Schmitz, O., Straatsma, M.W., Vannametee, E., Wisser, D., Bierkens, M.F.P., 2018. PCR-GLOBWB 2: a 5 arcmin global hydrological and water resources model. Geosci. Model Dev. 11, 2429−2453. https://doi.org/10.5194/gmd-11-2429-2018.

Sutanto, S.J., Wetterhall, F., Van Lanen, H.A.J., 2020. Hydrological drought forecasts outperform meteorological drought forecasts. Environ. Res. Lett. 15 (8), 084010. https://doi.org/10.1088/1748-9326/ab8b13.

Tallaksen, L.M., Stahl, K., 2014. Spatial and temporal patterns of large-scale droughts in Europe: model dispersion and performance. Geophys. Res. Lett. 41, 429−434. https://doi.org/10.1002/2013GL058573.

Taufik, M., Setiawan, B.I., Van Lanen, H.A.J., 2018. Increased fire hazard in human-modified wetlands in Southeast Asia. Ambio 48, 363−373. https://doi.org/10.1007/s13280-018-1082-3.

Todini, E., 1988. Rainfall−runoff modeling − past, present and future. J. Hydrol. 100, 341−352. https://doi.org/10.1016/0022-1694(88)90191-6.

Van den Besselaar, E.J.M., Klein Tank, A.M.G., Van der Schrier, G., Abass, M.S., Baddour, O., Van Engelen, A.F.V., Freire, A., Hechler, P., Laksono, B.I.I., Jilderda, R., Foamouhoue, A.K., Kattenberg, A., Leander, r., Martínez Güingla, R., Mhanda, A.S., Nieto, J.J., Sunaryo Suwondo, A., Swarinoto, Y.S., Verver, G., 2015. International climate assessment & dataset: climate services across Borders. Bull. Am. Meteorol. Soc. 1, 16−21. https://doi.org/10.1175/BAMS-D-13-00249.1.

Van Duinen, R., Filatova, T., Jager, W., van der Veen, A., 2016. Going beyond perfect rationality: drought risk, economic choices and the influence of social networks. Ann. Reg. Sci. 57 (2−3), 335−369. https://doi.org/10.1007/s00168-015-0699-4.

Van Emmerik, T.H.M., Li, Z., Sivapalan, M., Pande, S., Kandasamy, J., Savenije, H.H.G., Chanan, A., Vigneswaran, S., 2014. Socio-hydrologic modeling to understand and mediate the competition for water between agriculture development and environmental health: murrumbidgee River basin, Australia. Hydrol. Earth Syst. Sci. 18, 4239−4259. https://doi.org/10.5194/hess-18-4239-2014.

Van Huijgevoort, M.H.J., Hazenberg, P., Van Lanen, H.A.J., Teuling, R., Clark, D., Folwell, S., Gosling, S., Hanasaki, N., Heinke, J., Koirala, S., Stacke, T., Voβ, F., Sheffield, J., Uijlenhoet, R., 2013. Global multi-model analysis of hydrological drought in the second part of the 20th century (1963-2000). J. Hydrometeorol. 14, 1535−1552. https://doi.org/10.1175/JHM-D-12-0186.1.

Van Lanen, H.A.J., Prudhomme, C., Wanders, N., Van Huijgevoort, M.H.J., 2019. Future of drought. In: Iglesias, A., Assimacopoulos, D., Van Lanen, H.A.J. (Eds.), Drought: Science and Policy. Wiley Blackwell, pp. 69−92. https://onlinelibrary.wiley.com/doi/pdf/10.1002/9781119017073.

Van Loon, A.F., Van Huijgevoort, M.H.J., Van Lanen, H.A.J., 2012. Evaluation of drought propagation in an ensemble mean of large-scale hydrological models. Hydrol. Earth Syst. Sci. 16, 4057−4078. https://doi.org/10.5194/hess-16-4057-2012.

Van Loon, A.F., Van Lanen, H.A.J., 2012. A process-based typology of hydrological drought. Hydrol. Earth Syst. Sci. 16, 1915−1946. https://doi.org/10.5194/hess-16-1915-2012.

Van Loon, A.F., Van Lanen, H.A.J., 2013. Making the distinction between water scarcity and drought using an observation-modeling framework. Water Resour. Res. 49, 1483−1502. https://doi.org/10.1002/wrcr.20147.

Van Loon, A.F., Rangecroft, S., Coxon, G., Werner, M., Wanders, N., Di Baldassarre, G., Tijdeman, E., Bosman, M., Gleeson, T., Nauditt, A., Aghakouchak, A., Breña-Naranjo, J.A., Cenobio-Cruz, O., Costa, A.C., Fendekova, M., Jewitt, G., Kingston, D.G., Loft, J., Mager, S.M., Mallakpour, I., Masih, I., Maureira-Cortés, H., Toth, E., Van Oel, P., Van Ogtrop, F., Verbist, K., Vidal, J.-P., Wen, L., Yu, M., Yuan, X., Zhang, M., Van Lanen, H.A.J., 2022. Streamflow droughts aggravated by human activities despite management. Environ. Res. Lett. 17, 044059. https://doi.org/10.1088/1748-9326/ac5def.

Van Walsum, P.E.V., Veldhuizen, A.A., Groenendijk, P., 2010. SIMGRO 7.1.0, Theory and Model Implementation. Wageningen, Alterra, Wageningen, the Netherlands. Alterra-Report 913. http://content.alterra.wur.nl/Webdocs/PDFFiles/Alterrarapporten/AlterraRapport913.1.pdf.

Wada, Y., Van Beek, L.P.H., Wanders, N., Bierkens, M.F.P., 2013. Human water consumption intensifies hydrological drought worldwide. Environ. Res. Lett. 8 (3), 034036. https://doi.org/10.1088/1748-9326/8/3/034036.

Wada, Y., Bierkens, M.F.P., De Roo, A., Dirmeyer, P.A., Famiglietti, J.S., Hanasaki, N., Konar, M., Liu, J., Müller-Schmied, H., Oki, T., Pokhrel, Y., Sivapalan, M., Troy, T.J., van Dijk, A.I.J.M., Van Emmerik, T., Van Huijgevoort, M.H.J., Van Lanen, H.A.J., Vörösmarty, C.J., Wanders, N., Wheater, H., 2017. Human-water interface in hydrological modeling: current status and future directions. Hydrol. Earth Syst. Sci. 21, 4169−4193. https://doi.org/10.5194/hess-21-4169-2017.

Wanders, N., Wada, Y., 2015. Human and climate impacts on the 21st century hydrological drought. J. Hydrol. 526, 208−220. https://doi.org/10.1016/j.jhydrol.2014.10.047.

Wanders, N., Wada, Y., Van Lanen, H.A.J., 2015. Global hydrological droughts in the 21st century under a changing hydrological regime. Earth Syst Dyn. 6, 1−15. https://doi.org/10.5194/esd-6-1-2015.

Wanders, N., Thober, S., Kumar, R., Pan, M., Sheffield, J., Samaniego, L., Wood, E.F., 2019. Development and evaluation of a Pan-European multi-model seasonal hydrological forecasting system. J. Hydrometeorol. 20, 90−115. https://doi.org/10.1175/JHM-D-18-0040.1.

Warszawski, L., Frieler, K., Huber, V., Piontek, F., Serdeczny, O., Schewe, J., 2013. The inter-sectoral impact model intercomparison project (ISI−MIP): project framework. Proc. Natl. Acad. Sci. U. S. A. 111 (9), 3228−3232. https://doi.org/10.1073/pnas.1312330110.

Weedon, G.P., Balsamo, G., Bellouin, N., Gomes, S., Best, M.J., Viterbo, P., 2014. The WFDEI meteorological forcing data set: WATCH Forcing Data methodology applied to ERA-Interim reanalysis data. Water Resour. Res. 50, 7505−7514. https://doi.org/10.1002/2014WR015638.

Weiler, M., Beven, K.J., 2015. Do we need a community hydrological model? Water Resour. Res. 51 (9), 7777−7784. https://doi.org/10.1002/2014WR016731.

Wendt, D.E., Bloomfield, J.P., Van Loon, A.F., Garcia, M., Heudorfer, B., Larsen, J., Hannah, D.M., 2021. Evaluating integrated water management strategies to inform hydrological drought mitigation. Nat. Hazards Earth Syst. Sci. 21, 3113−3139. https://doi.org/10.5194/nhess-21-3113-2021.

Wens, M., Johnson, M.J., Zagaria, C., Veldkamp, T.I.E., 2019. Integrating human behavior dynamics into drought risk assessment—a sociohydrologic, agent-based approach. WIREs Water 6, e1345. https://doi.org/10.1002/wat 2.1345.

Wens, M., Veldkamp, T.I.E., Mwangi, M., Johnson, J.M., Lasage, R., Haer, T., Aerts, J.C.J.H., 2020. Simulating small-scale agricultural adaptation decisions in response to drought risk: an empirical agent-based model for semi-Arid Kenya. Front. Water 2 (15), 1−21. https://doi.org/10.3389/frwa.2020.00015.

Wisser, D., Fekete, B.M., Vörösmarty, C.J., Schumann, A.H., 2010. Reconstructing 20th century global hydrography: a contribution to the global terrestrial network- hydrology (GTN-H). Hydrol. Earth Syst. Sci. 14 (1), 1−24. https://doi.org/10.5194/hess-14-1-2010.

Wong, W.K., Beldring, S., Engen-Skaugen, T., Haddeland, I., Hisdal, H., 2011. Climate change effects on spatiotemporal patterns of Hydroclimatological summer droughts in Norway. J. Hydrometeorol. 12, 1205−1220. https://doi.org/10.1175/2011JHM1357.1.

Web references

URL 9.1 https://pdfs.semanticscholar.org/63bd/fae51662c0bc5e8227a0eaa9dbc521a55d30.pdf (Accessed: 14 June 2022).

URL 9.2 https://assets.publishing.service.gov.uk/government/uploads/system/uploads/attachment_data/file/290976/scho0308bnvz-e-e.pdf (Accessed: 14 June 2022).

URL 9.3 https://web.archive.org/web/20140521031412/http://www.geo.uzh.ch/en/units/h2k/services/hbv-model (Accessed: 30 December 2021).

URL 9.4 https://github.com/UU-Hydro/PCR-GLOBWB_model (Accessed: 10 June 2022).

URL 9.5 https://portal.grdc.bafg.de/ (Accessed: 10 June 2022).

URL 9.6 https://www.wur.nl/web/show/id=310672/langid=43 (Accessed: 13 June 2022).

URL 9.7 https://www.mikepoweredbydhi.com/products/mike-she (Accessed: 13 June 2022).

URL 9.8 https://parflow.org/ (Accessed: 13 June 2022).